1962

The oxidation of chromium diffusion coatings

Thomas Nilan Fogarty
Lehigh University

THE OXIDATION OF CHROMIUM DIFFUSION COATINGS

by

Thomas Nilan Fogarty

A Dissertation

Presented to the Graduate Faculty

of Lehigh University

in Candidacy for the Degree of

Master of Science

Lehigh University

1962

This thesis is accepted and approved in partial fulfillment of the requirements for the degree of Master of Science.

May 24 1962
(date)

Ralph Jacobsen
Professor in charge

H. Lukoff
Head of the Department

Acknowledgment

I wish to express my appreciation to Bell Telephone Laboratories and in particular J. E. Clark for support of this thesis. Discussions with K. E. Benson, J. Drobek, J. F. Libsch, and M. R. Notis were very rewarding. The helpful suggestions of R. G. Shankweiler and T. D. Jones in metallographic examination are greatly appreciated. I wish to thank Miss A. D. Mills for her help in x-ray powder diffraction. Special appreciation is due to D. Spang for his help in the experimental portion of this thesis. Also, appreciation is due to my wife Margaret for help in assembling the rough draft and to Mrs. M. R. Verostick for typing the final draft. Finally, A great debt is owed to R. J. Jaccodine for his advice and direction through the course of this thesis.

Table of Contents

	Page
1. Introduction	2
2. Chromium Diffusion Coatings	5
1. General Discussion	5
2. Physical Chemistry of Chromizing	6
3. Practical Chromizing Methods	9
4. Experimental Investigation of Structure of the Coatings	12
5. Discussion on the Structure of the Coatings	16
3. Review of Theories of Oxidation	20
1. General	20
2. Rate of Film Growth	21
3. The Adherence of Oxide Films	26
4. Oxidation of Chromium Diffusion Coatings	29
1. Experimental Investigation	29
2. Optical and X-ray Examination	32
3. Discussion	35
Conclusions	39
Bibliography	40,41
Biography	62

List of Figures

Page

Figure 1 - Variation with Temperature of the Equilibrium Constant for the Chromized Reactions (After T. P. Hoar & E. A. G. Groom[7]) 42

Figure 2 - Typical Time/Temperature Graph for a Chromizing Operation by the D.A.L. Process (After R. L. Samuel & H. A. Lockington[6]) 42

Figure 3 - Chromium-Molybdenum Binary Equilibrium Diagram (from ASM Metals Handbook 1948 Edition) 43

Figure 4 - Chromized Molybdenum Specimen (43X) Angle-Lapped at 1.25° Chrome Etched 44

Figure 5 - Chromized Molybdenum Specimen (43X) Angle-Lapped at 1.25° Molybdenum Etched 44

Figure 6 - Variation of Case Depth with Time and Temperature (After T. P. Hoar and E. A. G. Groom[7]) 45

Figure 7 - Polarized Light Photograph of Chromized Kovar Specimen (500X) Angle-Lapped at 1.25°, Chrome Etched 45

List of Figures, Cont'd.

Page

Figure 8 - Chromized Kovar Showing Grain Boundary Diffusion Dark Field Illumination of Chromized Kovar Specimen (500X) Angle-Lapped at 60°, Chrome Etched 46

Figure 9 - Chromized Kovar Showing Diffusion Layers, Specimen (250X) Angle-Lapped at 1.°, Chrome Etched 46

Figure 10 - Chromized Kovar Showing Diffusion Layers, Specimen (306X) Angle-Lapped 1.25°, Chrome Etched 47

Figure 11 - Protrusion of Chromized Kovar Specimen (25X) Angle-Lapped at 1°. Chrome Etched 48

Figure 12 - Surface in the Area of the Protrusion of Chromized Kovar Specimen (306X). No Etch 49

Figure 13 - Surface Outside the Area of Protrusion Chromized Kovar Specimen (306X). No Etch 49

Figure 14 - Surface Roughness Profile of Chromized Kovar 50

Figure 15 - Typical Experimental Oxidation Run 51

Figure 16 - Oxidation Rate of Chromized Kovar in Wet Hydrogen Atmosphere 52

List of Figures, Cont'd.

		Page
Figure 17 -	Oxidation Rate of Chromized Molybdenum in Wet Hydrogen Atmosphere	53
Figure 18 -	Idealized Curve of the Oxidation of Chromized Kovar Showing Sample Selection	54
Figure 19 -	Polarized Light Photomicrograph (~300X) of the Surface of the Oxide on Sample (1)	54
Figure 20 -	Polarized Light Photomicrograph (~300X) of the Surface of the Oxide on Sample (2)	55
Figure 21 -	Polarized Light Photomicrograph (~300X) of the Surface of the Oxide on Sample (3)	55
Figure 22 -	Photomicrograph (500X) of the Surface of the Oxide on Sample (2) (Showing Oxide Film Cracks)	56
Figure 23 -	Photomicrograph (500X) of the Surface of the Oxide on Sample (4) (Showing Healing of the Oxide Film)	56
Figure 24 -	Oxidation Rate of Chromium (After Gulbranson & Andrew[25])	57
Figure 25 -	Oxidation Rate of Type 446 Stainless Steel (After Caplan & Cohen[26])	57

List of Figures, Cont'd.

Page

Figure 26 - Oxidation Rate of Chromized Steel in Oxygen Atmosphere (After P. Galmiche[8]) 58

List of Tables

		Page
Table I	- Oxidation of Chromized Kovar	59
Table II	- Oxidation of Chromized Molybdenum	60
Table III	- Optical and X-ray Examination of the Oxidation of Chromium Diffusion Coatings	61

Abstract

The structure of chromium diffusion coatings on kovar (an iron-nickel-cobalt alloy used in glass to metal sealing) and molybdenum are studied by metallographic techniques and x-ray diffraction. Layered structures were observed in agreement with Rhines's Theory of diffusion coatings. The diffusion coating on kovar consisted of α, σ, and γ phases. It is believed that cobalt forms σ cobalt chromium and thus accelerates the normally sluggish transformation to σ iron chromium. The coating on molybdenum forms a single α chromium-molybdenum layer.

Oxidation rates of chromized coatings in wet hydrogen were determined by measuring weight gain of the specimens at various temperatures and times. Oxidation at 700°C was found to be space charge limited. Oxidation at temperatures greater than 900°C was sensitive to the substrate material. That is, the weight gain of chromized molybdenum was greater than that of chromized kovar.

At 1100°C oxidation of chromized kovar exhibits film cracking in the oxide. Film cracking is observed by optical means. The oxidation products are studied by x-ray powder diffraction. The major constituent is Cr_2O_3.

1. Introduction

The use of chromium diffusion coatings on iron and steel to provide resistance to high temperature oxidations and abrasion and wear resistance is well known. This process has commonly been called chromizing and has been discussed by Burns and Bradley[1] in connection with these applications. In general, chromized steels may be considered comparable in corrosion resistance to a thirty per cent chromium steel. The chromium steel is slightly preferable for wet corrosion. However, the chromized steel shows better resistance to oxidation at elevated temperatures. Modern chromizing technique generally involves the mechanism of gaseous transfer from some chromium source to the surface with solid state diffusion at the surface of the substrate resulting in alloy formation and a true metallurgical bond. Considering this process it is easy to rationalize the improved adherence of chromium diffusion coatings over hard chrome plating. In applications involving wear and abrasion resistance, maximum surface hardness is desired. Therefore, care must be taken to avoid decarburization of the steel to be coated if the maximum amount of chromium carbide is to be developed on the surface.

Another somewhat less known application of the chromizing process is the use of chromized coating to provide controlled oxidation in metal to glass sealing. Wachtell and Leighton[2] have described application of chromizing to glass to metal sealing. Many alloys, having optimum expansion characteristics for sealing to particular glasses, are ruled

out by the fact that the oxides of these alloys develop a weak interfacial bond between glass and metal. Chromium oxides have long been noted for excellent bonding to glass.

Partridge[3] points out the importance of the metal oxide in glass to metal adherence. The oxide having some degree of solubility in both glass and metal may act as a cement. In general, there are three important areas in glass to metal sealing. The first is a proper match with the coefficient of thermal expansion. The second is the strength of the interfacial bond between glass and metal, namely the adherence. This second factor is greatly influenced by the character of the metal oxide. The third factor is seal geometry.

Considering the above-mentioned factors in order the effect of chromizing on them is discussed. First when chromizing glass sealing metals, careful control of case depth is essential if undesirable changes in the thermal coefficient of expansion of the sealing metal is to be avoided. Diffusion from thick layers during subsequent high temperature operations would alter the properties of the substrate. Case depths of the order of 0.0005-0.001 inches do not substantially change the thermal coefficient of expansion of the substrate.

The second important factor modified by chromizing is the adherence between glass and metal. Fracture in a glass to metal seal generally occurs at the oxide-metal boundary

or in the glass itself. The adhesion between the glass and the oxide generally is very strong due to the ionic structure of both the metal oxide and the glass. It is easy to visualize a gradual change in these ionic structures with chromium ions displacing silicon ions in the glass. The adherence between the metal and the metal oxide is a more difficult problem and will be discussed later. Applications have centered around the desire for a more easily controlled oxidation or the improved adherence of chromium (III) oxide (Cr_2O_3) to glass. While chromium electroplates have been used to achieve the above results, the diffusion coating is preferable because of the improved adherence between the diffusion coating and the metal.

The third factor seal geometry has an important contribution to the residual stress of the seal but is not affected by chromizing. However, the seal geometry may greatly restrict the efficiency of the chromizing method. This restriction is discussed later in reviewing the practical chromizing methods.

One of the earliest applications of chromized coatings in glass to metal sealing was the use of chromized molybdenum. Molybdenum had been a difficult material to seal in air because of the formation of volatile oxides. By use of the chromized coating this undesirable feature has been eliminated. Another application is the use of chromized kovar in glass to metal sealing. The principal reason for this application is the improved adherence can be expected between the chromized coating and the glass.

With increased use of chromium diffusion coatings in glass to metal sealing, study of chromium diffusion coatings on various glass sealing metals and alloys such as molybdenum and kovar is necessary. Due to the importance of the oxide layer in glass to metal sealing, knowledge of the structure, composition and morphology of the oxide is of interest. The rate of oxide deposition and the possibility of film cracking such as exhibited by the stainless steels should be studied. Therefore this thesis has the following objectives:

1. An investigation of the structure of chromium diffusion coatings on molybdenum and kovar, (an iron-nickel-cobalt alloy).
2. An investigation of the oxidation of chromium diffusion coatings on the above-mentioned substrates.

2. Chromium Diffusion Coatings

1. General Discussion

Udy and Sully[4,5] devote parts of their monographs on chromium to a discussion of diffusion coatings. Early attempts at chromium diffusion coatings were by a powder cementation process analogous to sherardizing. The principal disadvantage of this method was the exceedingly high temperatures required. Chromizing by the cementation process was conducted at temperatures from 1300°-1400°C. These high temperatures impared the physical properties of a steel through excessive decarburization and grain growth. More modern processes have utilized a gaseous carrier to

transport the chromium to the substrate surface. Utilizing gaseous transfer processes, temperatures range from 800°-1100°C. These lower temperatures alleviate grain growth and decarburization.

Another important variation exists in chromizing for glass to metal sealing. Conversely to the wear resistant applications mentioned in the introduction, chromizing for glass to metal sealing is usually done on decarburized substrates. Chromium carbide is deleterious in glass to metal seals in two ways: First, the adherence of glass to chromium carbides is questionable. Second, the possibility of inconsistent oxidation and bubbles in glass to metal seals is present.

2. Physical Chemistry of Chromizing

Samuel and Lockington[6] have summarized the information concerning the physical chemistry of possible reactions in chromizing. Essentially, three possible reactions may take place at the surface of the substrate. They are: the replacement reaction, the reduction reaction, and thermal dissociation.

The replacement reaction on an iron surface may be written as

$$Fe + CrX_2 \rightleftarrows FeX_2 + Cr$$

where X represents a halide ion usually the chloride. As the above reaction is reversible, the equilibrium chromium concentration at the surface depends on the relative vapor

pressure of chromous and ferrous chlorides in the gas phase. However, even if the ferrous halides is efficiently removed, the rate determining factor of the forward reaction is dependent upon the iron in the surface. That is, the surface concentration of chromium will increase more slowly as the activity of the iron on the surface is reduced with a reduction in iron concentration at the surface. Because iron and chromium have substantially the same size and weight the replacement of iron by chromium does not affect the specimen size and weight.

Similarly the reduction reaction may be written as

$$H_2 + CrX_2 \rightleftarrows 2HX + Cr$$

and the thermal dissociation as

$$CrX_2 \rightleftarrows Cr + X_2$$

Both of these reactions are catalyzed by the surface and are additive to the surface, that is they increase the size and weight of the specimen.

In order to promote forward movement of all reactions, it is desired to maintain a high concentration of chromous chloride above the surface and to remove the products of the reaction.

Hoar and Groom[7] have shown that both interchange and reduction reactions are thermodynamically possible in a system where the halogen is restricted to chlorine. Variation of the equilibrium constant with temperature is

shown in Figure 1. Considering reactions of the following type

$$Cr + Cl_2 \rightleftarrows CrCl_2$$

$$Fe + Cl_2 \rightleftarrows FeCl_2$$

$$Mo + Cl_2 \rightleftarrows MoCl_2$$

$$H_2 + Cl_2 \rightleftarrows 2HCl$$

We have the following equilibrium constants (K)

$$K_{Cr} = \frac{P_{CrCl_2}}{A_{Cr} \times P_{Cl_2}}$$

$$K_{Fe} = \frac{P_{FeCl_2}}{A_{Fe} \times P_{Cl_2}}$$

$$K_{Mo} = \frac{P_{MoCl_2}}{A_{Mo} \times P_{Cl_2}}$$

$$K_{H} = \frac{P^2_{HCl}}{P_{H_2} \times P_{Cl_2}}$$

where P represents the partial pressure of the vapor and A represents the activity of substance. Then the equilibrium constant (K) of the replacement reaction with iron is

$$K_1 = \frac{K_{Cr}}{K_{Fe}} = \frac{P_{CrCl_2} \times A_{Fe}}{P_{FeCl_2} \times A_{Cr}}$$

or

$$\text{Log } K_1 = \log K_{Cr} - \log K_{Fe}$$

Similarly for the replacement reaction with molybdenum, we have the equilibrium constant K_2 given by

$$K_2 = \frac{K_{Cr}}{K_{Mo}}$$

or

$$\text{Log } K_2 = \log K_{Cr} - \log K_{Mo}$$

Now if valid assumptions are possible for activities through the chromizing process quantative predictions may be made. Considering (Figure 1) chromizing of iron by replacement is more probable than the chromizing of nickel or molybdenum. Also log K_H lies very close to log K_{Fe} so that the reduction reaction is equally probable. Following similar reasoning we see that while thermal dissociation of the iodies can supply chromium to the substrate surface. However, hydrogen iodide unlike hydrogen chloride and fluoride is readily dissociated at temperatures as low as 800°C curtailing the role of the reduction reaction in an iodide system.

3. Practical Chromizing Methods

Several methods have been used for chromizing and are summarized by Samuel and Lockington[6]. A brief discussion of these methods follows.

The first process to be discussed is the B.D.S. process which uses chromous chloride as the gaseous carrier and takes place in a reducing atmosphere. This process is

carried out in two stages. The first stage consists of activation of the chromizing compound. Ferrochromium is reacted with hydrogen chloride to form chromous chloride which is absorbed on the pores of a refractory material. After the activation is complete the chromizing compound is cooled in hydrogen. The second stage, the actual chromizing operation, packs the articles to be chromized in the activated compound and heats them to approximately 1050°C for several hours in a hydrogen atmosphere. Chromous chloride is volatized and the specimen is chromized by reduction and replacement reactions.

A second method of chromizing is salt bath chromizing. The bath consists of a salt mixture of approximately 30% chromous chloride. Flake chromium was introduced at the bottom of the crucible to replace chromium used in the reaction. A protective atmosphere over the bath was necessary because of the volatile salts. The advantages of this operation include a production of loading time and heat-up and cool-down time. Also parts requiring different lengths of treatment could be processed simultaneously.

A third process is the O.N.E.R.A. process which is a gaseous process involving fluoride as the active chromizing agent. In this process the parts are not packed in a chromizing mixture. One might expect better surface finish from this process. However, the ability of this process to chromize blank holes having a high depth to width ratio is questionable.

Another process somewhat simpler in technique is the D.A.L. process. This process is similar to pack carburizing. The parts to be chromized are dusted with a chromizing compound and packed into a retort which must prevent oxidation during heating and prevent an inrush of air during gaseous contraction upon cooling. The chromizing compound used in this process consists of a mixture of ferrochromium ammonium iodide and unvitrified kaolin powder. Ammonium ~~io~~dide dissociates upon heating forming ammonia and hydrogen iodide.

$$NH_4\ I \rightarrow NH_3 + HI$$

The ammonia then dissociates into hydrogen and nitrogen.

$$2NH_3 \rightarrow 3H_2 + N_2$$

Chromium iodide is then formed by the following reaction.

$$Cr + 2HI \rightarrow CrI_2 + H_2$$

Hydrogen iodide also undergoes a dissociation reaction.

The chromizing reactions are:

$$CrI_2 + Fe \rightarrow FeI_2 + Cr$$

$$CrI_2 + H_2 \rightarrow 2HI + Cr$$

also

$$FeI_2 + H_2 \rightarrow 2HI + Fe$$

Because of the instability of chromium iodide there is practically a complete regeneration of iodine derivatives upon cooling. This picture is modified for chlorides and

bromides as they form more stable salts and thus decrease the efficiency of the chromizing compound. Also the chlorides and bromides are deliquescent. A typical time temperature curve for the D.A.L. process is shown in Figure 2.

4. Experimental Investigation of Structure of the Coatings.

Two systems were examined experimentally. The first was chromized molybdenum. The second was chromized kovar. The molybdenum used in this experiment was 99.9% pure molybdenum with trace impurities of oxygen and nitrogen. The nominal chemical composition of the kovar is 53.7% iron, 29% nickel, 17% cobalt, and 0.3% manganese. Samples of kovar and molybdenum were prepared in the form of discs. These discs were blanked from 0.030 inch thick sheet and had a diameter of 0.625 inch. All samples were then degreased in trichloroethylene for 15 minutes followed by a 15 minute rinse in acetone. They were then ultrasonically cleaned in a solution of igepal (a nonionic detergent) then rinsed in grade (o) deionized water.

The specimens used in this work were chromized by the Chromalloy Corporation of West Nyack, New York.(3) The process used is one similar to the D.A.L. process described earlier. It is labeled a pack-chromizing process, but it should be remembered that the actual transfer is a gaseous one. The work is imbedded in a fine powder consisting of chromium or ferrochromium and an inert extender,

such as kaolin, to prevent sintering of the pack and an ammonium halide energizer. The case depth of the chromalloy coating was 0.001 inch on both the kovar and molybdenum samples.

After chromizing the degreasing and cleaning procedure discussed above was repeated. This was followed by baking the samples in dry hydrogen for one hour at 1100°C. This treatment, while desirable from the point of view of the oxidation studies, would tend to thicken the coating slightly and may have an effect on composition and structure (see Figure 6). As the diffusion of chromium in molybdenum is less than that of chromium in kovar, one might expect a slight variation in case depth between samples of kovar and samples of molybdenum. Part of these samples were then reserved for oxidation studies.

Chromized molybdenum samples were examined metallographically by angle-lapping. The case depth of the diffusion coating was approximately 0.0010 inch thick. The samples were etched to develop microstructure in a mixture of one part nitric acid, two parts glycerine, and three parts hydrochloric acid. First the glycerine and hydrochloric acid were mixed. This was followed by an addition of nitric acid and the solution was allowed to set for 5 to 10 minutes until a change in color from white to yellow was observed. The solution was then considered ready to use. When the solution became brown, it was

disregarded. This solution will hence be called chrome etch. Marble's reagent was also experimented with as an etch for the chromized diffusion coating, however, the chrome etch was found to be superior. Typical results of this etch are shown in Figure 4. The same sample was re-polished and etched with a solution of four parts concentrated hydrofluoric acid and one part concentrated nitric acid to develop the molybdenum microstructure. The results of this etch are shown in the photo-micrograph Figure 5. A single layer is observed which is identified as α chromium-molybdenum.

The second system studied was chromized kovar. The specimen was angle-lapped, chrome etched and observed metallographically under polarized light (see Figure 7). The intense green-yellow observed close to the surface is identified as clusters of nearly pure chromium. The same sample was observed under dark field illumination after chrome etching (see Figure 8), and grain boundary diffusion of chromium was observed.

The layers in the diffusion coatings of chromized kovar are shown in Figures 9 and 10. The absence of large areas of columnar ferrite structure is quite readily explained by the high nickel content of the substrate which stabilizes γ phase and the possibility of the σ phase growing at the expense of the columnar ferrite (α).

The chromized coatings were also studied by x-ray powder defraction. The sample was prepared by dissolving the kovar core from the diffusion coating in a forty per cent solution of concentrated nitric acid and distilled water. The residue was then powdered and exposed to 2-1/2 hours of chromium K α radiation using a Straumanis type Norelco camera. The results of this analysis indicate the major constituent was sigma iron chromium with the possibility of a mixture of sigma cobalt chromium and minor amounts of pure chromium and α iron. There was also some indication of nickel or a chromium nickel steel (chi phase).

During metallographic examination, an outward protrusion of the chromium coating was observed. This is a localized increase in thickness of the chromium coating giving a small raised area on the surface of the specimen. An angle-lapped cross section of the area is shown in Figure 11. Metallographic examination of the surface in the area of the protrusion and the immediately adjacent areas (Figures 12 & 13), show a larger grain size in the coating in the area of the protrusion. This area extends over several grain boundaries in the substrate. One might postulate growth in some preferred way. However, it cannot be demonstrated conclusively that this preferred growth is due to an inhomogeneity of the surface of the substrate or the chromizing method. Surface roughness of the samples was measured on a Taylor Hobson Talysurf Model 3 instrument. Typical

results are shown in Figure 14. In general, the surfaces of the samples could be described as a matte finish. Further discussion of surface finish will be deferred until the chapter on oxidation of the coatings.

5. Discussion on the Structure of the Coatings

Rhines[9,10] has pointed out that in diffusion coatings the layered structure may be explained as follows:

> "In binary systems, when diffusion occurs at a substantially constant temperature and pressure, the layers formed correspond in kind and in the order of their occurrence, to the single phase regions in the phase diagram at the temperature and pressure of diffusion; no two-phase layers appear. Layers corresponding to both the one and the two-phase regions appear in ternary systems. Stated in more general terms that apply to systems of all degrees of complexity: the layers formed by the isothermal and isobaric diffusion of metals across an interface correspond in kind and in the order of their occurrence to all regions in the phase diagram lying between the concentrations of the original bodies and having three or more degrees of freedom according to the phase rule (two or more degrees of freedom in the conventional temperature-concentration section where pressure is disregarded)."

Frame[11] discusses the order of appearance of layers in short-time diffusion. Essentially there are two views. One view is that all possible intermediate phases are present from the first instant of diffusion and that with increasing time these phases grow thicker until they are observed. As this is a diffusion control mechanism one would expect fastest growth in the beginning. But observation indicates that once an intermediate phase appears after a suspected incubation period the growth is relatively rapid. The other view postulates a nonequilibrium

interface. Essentially this consists of atom phases corresponding to the suspected intermediate phases. Possibly these phases appear via a nucleation and growth process. When one goes to long-time diffusion one may still not observe all the phases expected from the equilibrium diagram because even though time and temperature are sufficient for steady-state diffusion, it may be so slight that the layer will not reach an observable thickness. Considering the chromium-molybdenum equilibrium diagram (see Figure 3) and Rhines's Theory one would expect a single layer in chromium diffusion on molybdenum. Metallographic investigation of this system shows agreement with Rhines's Theory as a single layer of α chromium-molybdenum was observed. (See Figures 4 & 5.)

However the chromium diffusion coating on kovar is a much more complex system. Verification of Rhines' theories in this system would be extremely difficult because of the lack of information on the quaternary system (iron, nickel, cobalt, and chromium). In general, one would expect one-, two-, and three-phase regions to be present as layers.

In the analysis of the results of chromium diffusion on kovar coating, several factors should be kept in mind. First, prior to chromizing, the kovar samples were decarburized. Therefore one would expect the content of chromium carbides in the coatings to be neligible. Second, the high nickel content of the kovar alloy tends to stablize

the austenitic (γ) phase and thus would increase the quantity of chromium that is required to produce the α phase at the surface. Third, these parts were given a dry hydrogen bake at 1100°C for one hour. This treatment may modify the structure.

In addition to the method by which chromium is supplied to the surface, the thickness and composition of the chromized coating also depends on the rate of diffusion of chromium into the underlying metal. The composition at the surface depends upon the balance between the rate of chromium supplied to the surface by the various reactions and the rate at which it diffuses into the substrate. It should be noted that in turn the reaction rate of supply of chromium to the surface is affected by chromium content of the surface. In chromized coatings on mild steel,[5] a columnar ferrite (α) structure is observed. In steel this is due to a recrystallization to the ferrite structure at approximately 12 to 13 per cent chromium. At the temperature of the coating, the γ phase is formed. This may only partially transform leaving some retained austenite in the room temperature structure. Also, in the mild steel chromium coating a σ phase of complex lattice structure exists. This phase occurs at approximately 40 to 45 wt. per cent chromium and is bounded on both sides by a two-phase $\alpha + \sigma$ region which would occur in a binary system as interfacial lines. In mild steel,

the σ phase is formed by a very sluggish transormation and is generally not observable in the coatings.

Combining the metallographic analysis and the x-ray defraction analysis discussed in the experimental section, one could postulate the following order of layers; first, on the surface, one would expect mixture of clusters of pure chromium and chromium enriched α ferrite. The columnar ferrite structure is probably not observed because a great deal of it has transformed to σ iron chromium. Foley and Krivobok[13] have discussed σ formation in a nickel chromium iron system. Possibly σ cobalt chromium aids in the transformation. The σ cobalt chromium forms at a relatively high temperature and is a much less sluggish transformation. Thus one might expect that the cobalt content has a marked effect on the appearance of the σ phase in the diffusion coating. The σ phase is brittle and should be avoided if possible. As the chromium content is lowered below the σ phase, the action of nickel in stabilizing austenite should become a controlling factor and distinction between the γ phase of the diffusion coating and the substrate kovar would be difficult. The presence of a nickel-rich layer was not observed metallographically although in oxidation of kovar, another diffusion controlled process, this layer has been well established by metallographic technique.

T. C. Loomis[12] of Bell Telephone Laboratories, Murray Hill, has studied the chromium content of chromized coatings on mild steel via the electron microprobe analyzer. While surface contents of chromium have generally been described at a limit of 60 to 70 per cent chromium, Loomis has found clusters of pure chromium at, and near the surface. He has also traced high chromium content in the grain boundaries showing significant grain boundary diffusion. The layered structure discussed above was confirmed with a region in the 40 to 45 wt. per cent composition range leading one to expect that some σ phase was present. Metallographic work on chromized kovar discussed earlier is in agreement with Loomis' findings. That is, pure chromium clusters were observed at the surface (see Figures 7 & 10), and grain boundary diffusion of chromium was observed (see Figure 8).

The protrusions in the chromized coating is due to preferred growth of these pure chromium clusters. However, the mechanism for this preferred growth is not yet understood. Further experimentation is necessary in this area.

3. Review of Theories of Oxidation

1. General

Hauffe[14,15] has recently reviewed the theories of oxidation. Books by Kubaschewski and Hopkins,[16] and Evans[17] amply review not only the theory but report much of the experimental data on various elements and alloys.

Waber[18] has reviewed the kinetics of oxidation especially in high velocity gas streams such as encountered in supersonic flight. Wagner[19,21] has reviewed the importance of diffusion in the growth of thick films and methods for testing and evaluating observations in oxidation studies. The brief review presented in this chapter is not intended to be comprehensive or even cover all major points of oxidation theory. In general, only the areas which have a more or less direct bearing on the problem under study are considered.

The gas phase corrosion of metals consists of the formation of oxide, halide or sulfide layers. If these layers are very adherent to the metal, the films will tend to be protective and retard the rate of further reaction. However, if at a given temperature the rate of film growth remains high or if the film breaks away from the substrate exposing fresh metal, corrosion will proceed. The problem must then consider two areas. One is the factors influencing adhesion while the other is the mechanism of film growth.

2. Rate of Film Growth

The major empirical growth laws for oxidation are the parabolic, linear, logarithmic and cubic relationships between weight gain and time, at a given temperature. If the scale is nonporous, adherent and relatively thick, the process is usually diffusion limited and the parabolic

rate law is obeyed.

$$m^2 = Kt$$

In the rate equation m represents the weight gain of the specimen, and t represents the time of oxidation. K represents a constant that is particular to the material being oxidized and the temperature at which oxidation takes place.

As the thickness of the oxide layer increases, the diffusion resistance is increased and the reaction slows down. The rate constant K may be increased by increasing the temperature.

At thin film thicknesses a space charge may oppose the migration of ions. Thus, diffusion is retarded and the logarithmic growth law is followed

$$m = K \log (at+1)$$

where K and a are constants for a particular material and test temperature. At somewhat higher temperatures (above 325°C), the space charge region would have a lessened effect in retarding diffusion, then the cubic law holds

$$m^3 = Kt \quad .$$

Wagner[19] has developed a theory for a parabolic rate of oxidation as follows. In the relatively thick films, the rate of oxidation is directly proportional to the thickness of the oxide layer. Electroneutrality holds. The process is diffusion controlled and the reaction would

obey Fick's law giving the increase of thickness ΔX per unit time.

$$\frac{d\ (\Delta X)}{dt} = \frac{K}{\Delta X}$$

upon integration

$$\Delta X^2 = 2Kt$$

or rewriting in terms of weight gain

$$\left(\frac{\Delta m}{A}\right)^2 = 2Kt$$

In discussing diffusion controlled reactions, it is well to remember that there are several types of defects of importance. In stoichiometric crystals, these are the well-known Frenkel defects and Schottky defects. However, in ionic crystals differing from the stoichiometric composition, there exist cation vacancies and electron holes. Essentially, the oxides may then be divided into semiconductors.

In applying Wagner's Theory we must distinguish between the oxidation process in which the oxide layer is mainly an ionic conductor and those in which it is an electronic conductor. In the latter case we must distinguish between hole conduction and electron conduction. The formation of Cr_2O_3, Cu_2O, etc. is an oxidation process involving deficit semiconductors. In Cr_2O_3 the rate is limited by the diffusion of chromium ions via vacancies.

Wagner assumes that ions and electrons migrate independently and derives the following expression

$$\frac{Nequ}{A} = K_r \frac{1}{\Delta X}$$

where $\frac{Nequ}{A}$ is the rate of outward migration of the metal ions and the inward migration of the oxygen ions. The change in thickness is represented by ΔX. The rational rate constant K_r is dependent upon the conductivity of the oxide, the chemical potential, and the transport numbers of the ions and electrons. However by use of Einstein's relation to the rational rate constant may be expressed in terms of self-diffusion coefficients.

Mott[22] then rationalized the application of the various empirical rate laws to oxidation processes as follows. At high temperatures if a protective film is formed, the process is diffusion controlled and the parabolic law is obeyed. At somewhat lower temperatures, space charge effects begin to interfere and the cubic growth law is followed. A possible exception to this rule is the reported cubic growth of zirconium at high temperatures. At still lower temperatures the space charge effect becomes more pronounced. If migration of positive ions is slow, compared with that of electrons, and anions do not diffuse, the positive ions pile up resulting in a positive field which is the space charge. This space charge then opposes further migration,

diffusion is retarded, and the logarithmic law is followed. In these very thin films, the rate of migration of ions is no longer proportional to the field strength that is, no longer inversely proportional to the thickness of the film, but depends quasi-exponentially on the thickness. While Mott's theories take into account the existence a single space charge at the oxide metal interface, Wagner has pointed out that there is the possibility of an overlapping of two space charges, one at the oxide-metal interface and the other at the oxide-oxygen interface. This would give another interpretation to the logarithmic law especially for films thicker than 100 Å. Another theory differing from both Mott and Wagner in thin films is that Hauffe[14] and Engle which takes into account dependence on the pressure of oxygen. If the oxide layer formed is not adherent and coherent, oxidation occurs at much higher rate and follows a linear law

$$m = Kt \quad .$$

This law would be followed if a porous film is formed or if the film fractures at some critical thickness. Another case in which oxidation is controlled not by diffusion but by the rate of reaction at the oxide-oxygen interface also follows the linear law. At very high temperatures, oxidation occurs at the linear rate discussed above. However, there is a possibility that the oxidation rate at high temperatures may actually be smaller than the oxidation rate at slightly lower temperatures due to a sintering of the oxide film.

3. The Adherence of Oxide Films

The problem of the adherence of metal oxides is a difficult one and is essentially the problem of epitaxy. Seifert[23] has reviewed the problem of epitaxy especially Frank and van der Merwe's theory which indicates that there is a critical percentage of misfit about 10 to 20 per cent below which monolayer formation and subsequent strained growth occurs and above which discrete nuclei will grow with intermittent regions of noncontact. If these strained films grow they will eventually reach a thickness at which slip or recrystallization brings about normal lattice parameters. Very thin surface layers formed on metals are generally compact, adherent and pore-free. This has been observed even when the molar volume of the reaction product is less than the atomic volume of the metallic phase in contrast to the Pilling and Bedworth[14] rule which states that if the ratio of the molar volume of the reaction products and the molar volume of the metal is greater than one, compact surface layers are expected. The volume ratio does indeed play a role in the case of thicker films, but not as decisive as once thought. Some degree of accommodation in the oxide layer is necessary for compact formation of an oxide. Thus the readiness of both the metal and the oxide to undergo plastic deformation and some elastic deformability of the lattice is of great importance. The shrinkage in the metallic phase is by vacancy emission at dislocations. However, shrinkage in the oxide phase can

only be explained by diffusion of oxygen ions as well as metal ions which is a much slower process. In general, metals may form compact films by the inward movement of oxygen resulting in high stresses in the film. Compact films may also be grown by the outward movement of metal, a process which sometimes leaves cavities at the base of the film. Sometimes films are both stress free and cavity free possibly due to a balance in some way of the outward movement of the metal and inward movement of oxygen. In general, several mechanisms for rupture are apparent. A thick film is more liable to damage than a thin film and if the coefficient of expansion of the oxide and the metal differ greatly, detachment may occur upon cooling. In a simple case for smooth interface between metal and oxide, the work of detachment, Wa, is independent of the thickness while the total strain energy is proportional to the thickness, y, and may be written Cy. Therefore the critical thickness of detachment, due to the thermal coefficient of expansion differences, is given by the following formula:

$$y > Wa/C \ .$$

Also, cracking may occur when the strained lattice returns through slip or recrystallization to the normal lattice parameters. Metals such as chromium and nickel show a sudden speed-up in oxidation rate in several thicknesses. This will be discussed more fully in the following chapter. Another explanation for breakdown of parabolic growth is

that a thin layer of one oxide is formed followed by an additional layer of non-adherent, non-coherent oxide. Tungsten is a good example where the initial film is the dense W_4O_{10} and a powder WO_3 exists on top of it. After some period of parabolic growth, thickening of the first layer almost ceases and the oxidation rate becomes constant as it is not impeded by the powdery second layer.

While unchecked internal oxidation along grain boundaries may cause severe damage, it may if suitably controlled improve the adhesion of the main scale by "pegging-in". Careful control of "pegging-in" is necessary if the substrate is not to be greatly weakened by internal oxidation. The Nimonic alloys, which are nickel chromium alloys, have had exceptional success in the use of this principle to form more adherent oxides.

Gwathmey[20] has discussed the effect of orientation on oxidation. While most oxides have oxidation rates varying with orientation, chromium is somewhat of an exception in that its oxidation is independent of crystal orientation.

Before leaving the review of oxidation, some consideration should be given to the effect of second constituents. These may affect the oxidation rate in two ways. First, the second constituent may enter the film either increasing or decreasing defects in the films thus speeding up or retarding oxidation rates. A second mode of operation of

the second constituent is that it may accumulate at the base of the oxide film and increase the diffusion resistance thus retarding oxidation.

As mentioned earlier, this review is not expected to be comprehensive but merely to highlight some important aspects of oxidation which are useful in explaining the phenomena under study in the oxidation of chromium diffusion coatings. The reviews and books mentioned earlier in this chapter discuss the subject more fully and include many references to original work.

4. Oxidation of Chromium Diffusion Coatings

1. Experimental Investigation

Chromium diffusion coatings were prepared by the Chromalloy Corporation by the method discussed earlier. The case depths of these coatings were 0.001 inches. Coatings were on molybdenum and kovar (iron, nickel, cobalt alloy). The surface after chromizing had a matte finish. The surface roughness and evidence of protrusions have been presented earlier in this work. All samples were first degreased in trichloroethylene for 15 minutes followed by a 15-minute rinse in acetone. They were then ultrasonically cleaned in a solution of igepal (a non-ionic detergent) then rinsed in grade (o) deionized water. Following this treatment, they were baked in dry hydrogen for 1 hour at 1100°C. The above treatments were given to insure a uniform, chemically cleaned surface. The effects of surface roughness

on surface area would be expected to have the greatest effect in early stages of film growth or on very thin films. While the real surface area of a matte finish might be several times that of an electrolytically polished specimen, its effect would become less as oxidation proceeds due to a smoothing out action on the surface of the specimen, thus as the films becomes thicker the effect of surface roughness on rate of oxidation is less. Details of the geometry of the disks used as oxidation samples were discussed earlier in the chapter on chromium diffusion coating.

In this experiment, chromized kovar and chromized molybdenum were oxidized in an atmosphere of wet hydrogen saturated in water vapor at 23°C. This atmosphere is highly selective to chromium oxidation. The specimens were loaded into a retort brought up to temperature in a nitrogen atmosphere and then wet hydrogen was introduced into the system. After a specified period of oxidation time the system was flushed with nitrogen and the parts were cooled to room temperature in nitrogen. This operation was carried out in a Lindbergh vertical retort furnace. The time period of oxidation was counted from the beginning of hydrogen burnoff to the end of hydrogen burnoff. While there may be some small error in arriving at the exact time that oxidation begins and ends, the error at the beginning is self-compensating with the error

at the end. A typical oxidation run is shown in Figure 15.

The measurement of weight gain was carried out on a Mettler Grammatic Balance. The readability of this instrument is as indicated xx.xxxxx grams. Two samples were run at each condition of time and temperature. The average weight per square centimeter was then calculated. A sample calculation follows:

Time of oxidation - 6 minutes

Temperature of oxidation - 1100°C

	Sample A	Sample B
Weight after dry hydrogen bake-out in gms.	1.20110	1.24673
Weight after oxidation in gms.	1.20168	1.24730
Weight difference in mg.	.58	.57

Surface area of the sample was 4.31 square cm.

Weight gain (mg/sq. cm)	.1341	.1321
Ave. weight gain $\frac{\Delta m}{A}$ (mg/sq. cm)	.133	-

The data for the oxidation of chromized kovar is presented in Table I. The data is tabulated in columns of constant temperature. Similarly the data on chromized molybdenum is presented in Table II. Oxidation rate curves were then drawn from the above data. The average weight gain is plotted as a function of time at a constant temperature. The curves for the oxidation of chromized kovar are presented in Figure 16 while those for the

oxidation of chromized molybdenum are presented in Figure 17. A break was observed in the oxidation curve of chromized kovar at 1100°C. In order to examine the possibility of film cracking, samples from this particular curve were studied by optical and x-ray diffraction methods. Further consideration of oxidation rates will be deferred to the discussion.

2. Optical and X-ray Examination

Samples taken at points indicated in Figure 18 were examined both metallographically and by x-ray diffraction to ascertain the oxidation products and the effect of film cracking. First, the surface of these samples was examined by polarized light microscopy and normal metallurgical microscopy.

The same samples were then examined by x-ray diffraction. For the x-ray diffraction work, the oxide was removed from the surface by scraping. The samples were then powdered and analyzed by the powder-diffraction technique discussed earlier. Gulbranson, Phelps and Hickman[24] have discussed electron diffraction, electron microscopy and compared this with x-ray diffraction results on oxides. One difficulty that they have pointed out is the problem in differentiating between similar oxide structures such as α Fe_2O_3 and Cr_2O_3 especially if there is a possibility that these may be present as solid solutions of one another. Both Cr_2O_3 and

α Fe_2O_3 are rhombohedral structures with lattice parameters of 5.35 and 5.42 respectively. There is also a problem in differentiating between the various spinel-type oxides. In this structure there is a possibility of random replacement of ferric ions by chromium ions in a spinel such as Fe_3O_4.

The results of this experimental investigation are summarized in Table III using the specimen designation outlined in Figure 18. Sample 0 is the unoxidized chromium diffusion coated kovar examined in the chapter on diffusion coatings. Sample (1) is taken as soon as the relatively flat portion of the first parabola is reached. An examination of the surface via polarized light microscopy (see Figure 19) shows a fairly uniform green-blue surface indicative of Cr_2O_3. No breaks in the oxide are observable. X-ray diffraction analysis showed the oxide to be primarily Cr_2O_3, however, the possibility that a mixture of Cr_2O_3 and α Fe_2O_3 cannot be distinguished must be kept in mind. Present as a minor constituent in this first sample was CrO_2. Sample (2), taken immediately after the break in the oxidation curve was examined by polarized light microscopy of the surface (see Figure 20). Here the cracks are clearly present in the green field of Cr_2O_3. The purple spot forming in one of the cracks could be interpreted as a preferential growth of some second phase such as α Fe_2O_3 or a spinel probably of the type $FeOCr_2O_3$. Figure 22 is the same sample with its surface examined by normal metallurgical microscopy. The channel-

like fissures in the oxide are clearly present. X-ray diffraction analysis of this sample showed only Cr_2O_3 or the possibility of the mixture Cr_2O_3 plus α Fe_2O_3. However, this does not rule out the possibility of a spinel beginning to grow in the channels, as the quantity of the spinel would probably be below the minimum detectable limit via x-ray powder diffraction. It should be noted that a minor constituent CrO_2 is no longer present, but has probably transformed to Cr_2O_3. Sample (3) is taken at the time when the second flat portion of the curve is reached. Here the polarized light metallography indicates the green background with the blue growth in the channels. At this point it should be noted that the more bluish cast of Figure 19 and Figure 21 as compared with Figure 20 is of no real significance. The purple of Figure 20 corresponds to the blue of Figure 21 while the bright green of Figure 20 corresponds to the green with a bluish cast of Figure 21. These differences exist mainly because of the difficulty in establishing the same lighting and similar color photography on successive days. In sample (3), the suspected phase present only in spots in the channel in sample (2) has now grown throughout the channels. However, x-ray diffraction analysis shows no change from sample (2) to sample (3). Again one should note that the minimum detectable limit for this

technique as applied here is approximately 10 per cent for identification of minor constituents. Sample (4) which is taken after a long time on the second flat of the oxidation curve was examined by normal metallographic microscopy and the channel-like fissures were shown to be completely healed over. (See Figure 23.)

3. Discussion

In discussing the oxidation rate curves it is interesting to look first at temperature variation. At 700°C the oxidation of both the chromized molybdenum and chromized kovar specimens were very similar. Interference colors were observed in both cases. Therefore one would expect the thickness of these oxide films to be less than 2000 Å. In these thin films the effect of the space charge in retarding diffusion would certainly be expected.

At 900°C a great deal of scatter in the data was apparent. This is probably due to the fact that a critical temperature was reached. This point will be considered later in a discussion of film cracking of Cr_2O_3.

There is a promounced difference in the weight gain between chromized kovar and chromized molybdenum. This difference in the weight gain and the extremely good adherence of the chromized molybdenum oxide leads one to postulate a reaction between a normally volatile molybdenum oxide and chromium (III) oxide Cr_2O_3. At furnace temperatures, the most stable oxide of molybdenum MoO_3 is volatile. Possibly one might expect something

akin to liquid phase sintering. Evans[17] has discussed the catastrophic oxidation of molybdenum and the effect of chromium in reducing this.

At 1100°C the oxidation of chromized kovar exhibits a break in the oxide film and it appears that the parabolic rate constant has been raised as expected by temperature. Variability of the data in the second flat increased over that in the shorter time duration portions of the curve. However, the experimental technique used here would indicate a greater variability in the earlier portions of the curve. This increase in variability may be explained by the healing of the channel-like fissures by a second phase. If one considers that the effect of the coefficient of expansion of the substrate kovar which is 4.6×10^{6} inches per inch and the oxide Cr_2O_3 which is 8.2×10^{6} inches per inch, one could expect possible cracking due to strain energy from this mismatch upon cooling. However, while this may intensify the cracking it cannot serve to explain the break in the oxidation curve. The method by which the curves were obtained did not involve the temperature difference necessary for this effect to be of importance. One might also expect some accommodations on the basis of epitaxial considerations, that is, the strained lattice may revert to the normal lattice parameter causing a crack. Disappearance of CrO_2 after the break in the oxidation curve indicates a change in composition which may be instrumental in causing a crack.

Gulbranson[25] has explained film cracking on pure chromium in the following way: At high temperatures, the rate of evaporation may approach or equal the rate of oxidation. This sudden kinetic change may then bring about loss of adhesion on a localized basis accounting for film cracking. The thickness of the oxide is fairly important in this balance and Gulbranson has reported that the first break for pure chromium occurs at 4800 Å (see Figure 24) or .08 milligrams. This is in good agreement with the experimental data of the break on chromium diffusion coated kovar which also broke at .08 milligrams. If one assumes pure Cr_2O_3, the breaks would be identical. Also as the temperature at which evaporation becomes important is approximately 900°C, this may tend to explain the extreme variability in the oxidation data at that temperature.

Similar evidence of film cracking is exhibited in stainless steels discussed by Caplan and Cohen[26]. They reported oxidation products consisting primarily of Cr_2O_3 and various spinels and silicates (see Figure 25).

Thus chromium diffusion coatings seem to have oxidation characteristics somewhat between that of pure chromium and high chromium content alloys. One would expect that at the shorter times involved in oxidizing for glass to metal sealing, the oxidation characteristics would be more closely represented by the data for pure chromium. This fact was borne out in the investigation.

At longer times, one would expect oxidation properties more akin to the chromium-rich alloys. As depletion of chromium at the surface takes place, diffusion of other metals from the substrate may account for complex mixtures of metal oxides and spinels. An example of this is the work of Galmiche,[8] who has investigated the oxidation rate of chromized mild steel in an oxygen atmosphere. His work was carried out over longer time periods and in a more strongly oxidizing atmosphere. Figure 26 presents his data.

Conclusions

1. The sigma phase of iron chromium or cobalt chromium mixed with iron chromium was found present in chromium diffusion coatings on kovar. It is believed that the cobalt content of the substrate tends to accelerate this normally sluggish transformation to the brittle tetragonal sigma phase. Normally this transformation has not been a problem in chromized steel coatings.

2. Oxidation of chromized coatings in wet hydrogen at 700°C is space charge limited.

3. The weight gain of the chromized diffusion coating is dependent on the substrate material.

4. At higher temperatures, chromized diffusion coatings exhibit film cracking.

Bibliography

1. Burns, R. M. and Bradley, W. W., Protective Coatings of Metals, American Chemical Society Monograph Series, New York: Reinhold Publishing Corporation, 1955, pp. 229-234.

2. Wachtell, R. and Leighton, H. W., "Metal Diffusion Techniques", Electrical Design News, November, 1961.

3. Partridge, J. H., Glass-to-metal Seals, Scheffield: Society of Glass Technology, 1949, pp. 200-220.

4. Udy, Marvin J., Chromium, American Chemical Society Monograph Series, Volume II, New York: Reinhold Publishing Corporation, 1956, pp. 93-98.

5. Sully, A. H., Chromium, London: Butterworth Scientific Publications, 1954, pp. 157-222.

6. Samuel, R. L. and Lockington, N. A., "The Protection of Metallic Surfaces by Chromium Diffusion", Metal Treatment, Volume 18, (1951), pp. 354ff, 407ff, 440ff, 495ff.

7. Hoar, T. P. and Groom, E. A. G., "Thermodynamics of Chromizing Reactions", Journal of Iron St. Inst., Volume 169, (1951), p. 101.

8. Galmiche, P., "Nouveau procede de chromage thermique et formation d'alliages mixtes de diffusion", Revue de Metallurgie (3), Volume XLVII, 1950, pp. 192-198.

9. Rhines, F. N., "Diffusion Coating on Metals", Surface Treatment of Metals, Cleveland: American Society for Metals, 1941.

10. Rhines, F. N., Phase Diagrams in Metallurgy, New York: McGraw-Hill Book Company, Inc., 1956, pp. 107-109, 156-157.

11. Frame, J. W., "A Study of the Mechanism Controlling the Presence and Relative Thickness of Alloy Layers in Iron-Aluminum Diffusion Couples". Unpublished Ph.D. Dissertation, Lehigh University, 1961, pp. 4-16.

12. Loomis, T. C., "Electron Probe Analysis of Chromium Diffusion Coatings". Private communication.

13. Foley, F. B. and Krivobok, V. N., "Sigma Formation in Ni-Cr-Fe Alloys", Metal Progress, Volume 71, #5, pp. 81-86.

14. Hauffe, Karl, "The Mechanism of Oxidation of Metals and Alloys at High Temperatures", Progress in Metal Physics, Volume IV, pp. 71-104.

15. Hauffe, Karl, "On the Mechanism of the Oxidation of Metals", Surface Chemistry of Metals and Semiconductors, Edit., Gatos, New York: Wiley, 1960.

16. Kubaschewski, O. and Hopkins, B. E., Oxidation of Metals and Alloys, 2nd Edition, New York: Academic Press Inc., Publishers, 1962.

17. Evans, U. R., The Corrosion and Oxidation of Metals, London: Edward Arnold (Publishers) Ltd., 1961.

18. Waber, J. T., "Kinetics of Oxidation in a Gas Stream", Metals for Supersonic Aircraft and Missiles, Cleveland: American Society for Metals, 1958, pp. 96-169.

19. Wagner, C., "Diffusion and High Temperature Oxidation of Metals", Atom Movements, Cleveland: American Society for Metals, 1951, pp. 153-173.

20. Gwathmey, A. T. and Lawless, K. R., "The Influence of Crystal Orientation on the Oxidation of Metals", Surface Chemistry of Metals and Semiconductors, Edit., Gatos, New York: Wiley, 1960.

21. Wagner, C., "Methods of High Temperature Oxidation Testing and Evaluation of Observations", High Temperature Properties of Metals, Cleveland: American Society for Metals, 1950.

22. Mott, "A Theory of the Formation of Protective Oxide Films on Metals", Transactions of the Faraday Society, Volume 35, 1939, p. 1175ff, Volume 36, 1940, p. 472ff, Volume 43, 1947, p. 429ff.

23. Seifert, "Epitaxy", Structure and Properties of Solid Surfaces, Chicago: University of Chicago Press, 1953, pp. 318-383.

24. Gulbranson, Phelps and Hickman, "Oxide Films Formed on Alloys at Moderate Temp., Electron Diffraction and Electron Microscope Study", Industrial and Engineering Chemistry Analytical Edition, Volume 18, p. 640ff.

25. Gulbranson, Andrew, "Kinetics of the Oxidation of Chromium", Journal of the Electrochemical Society, Volume 104, pp. 334-338.

26. Caplan and Cohen, "High Temperature Oxidation of Some Iron-Chromium Alloys", Journal of Metals, Volume 4, pp. 1057-1065.

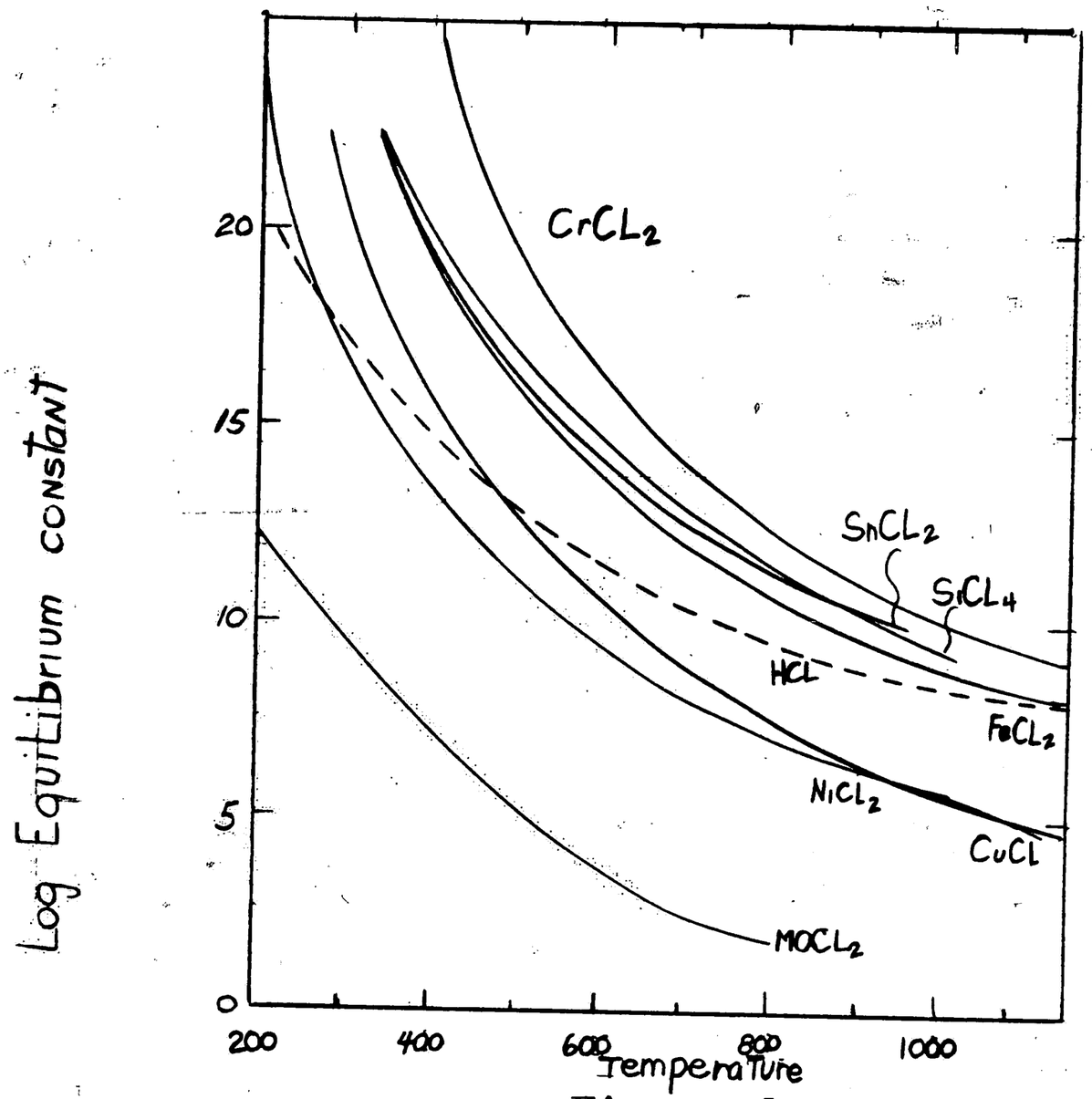

Figure 1

Variation with Temperature of the Equilibrium Constant for the Chromizing Reactions (After T. P. Hoar & E. A. G. Groom[7])

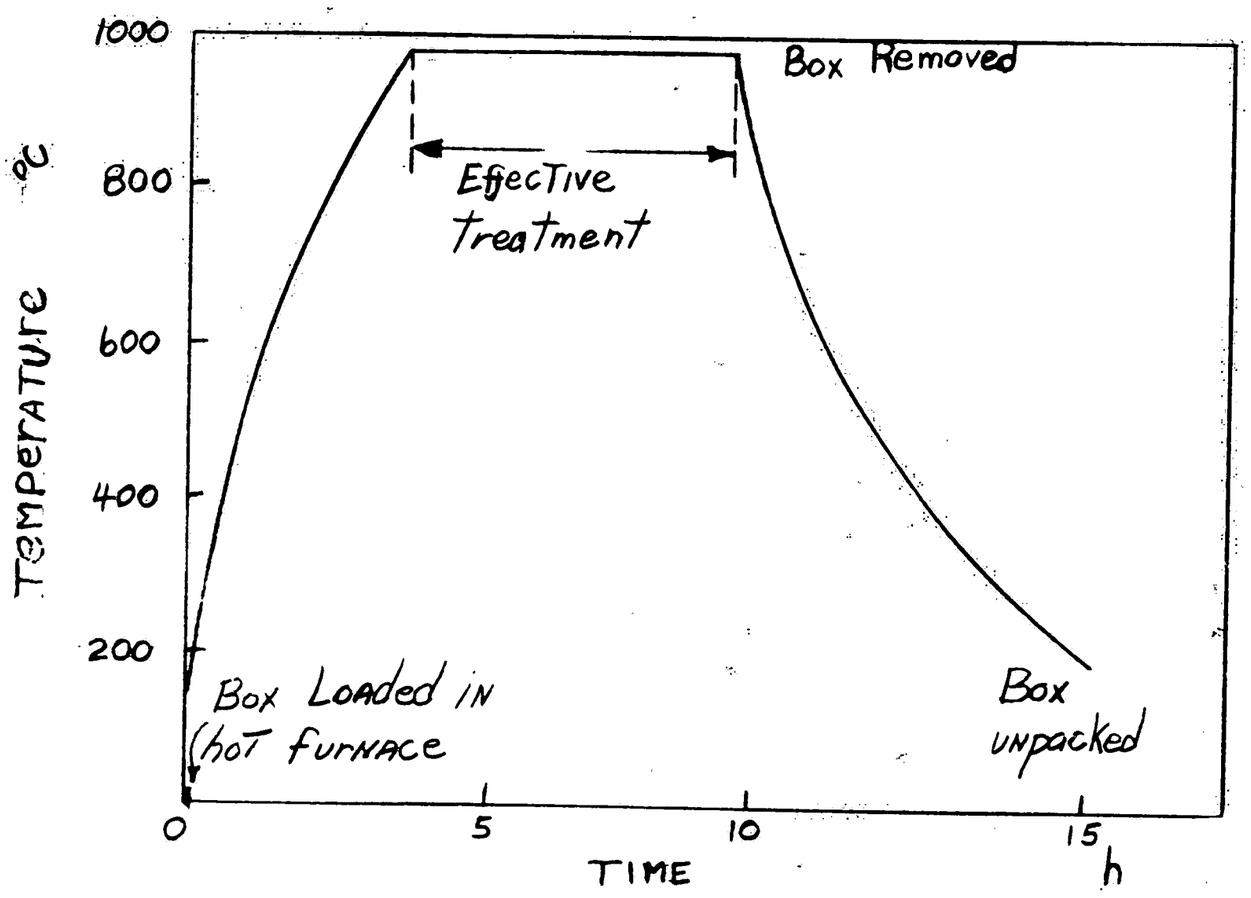

Figure 2

Typical Time/Temperature Graph for a Chromizing Operation by the D.A.L. Process (After R. L. Samuel & H. A. Lockington[6])

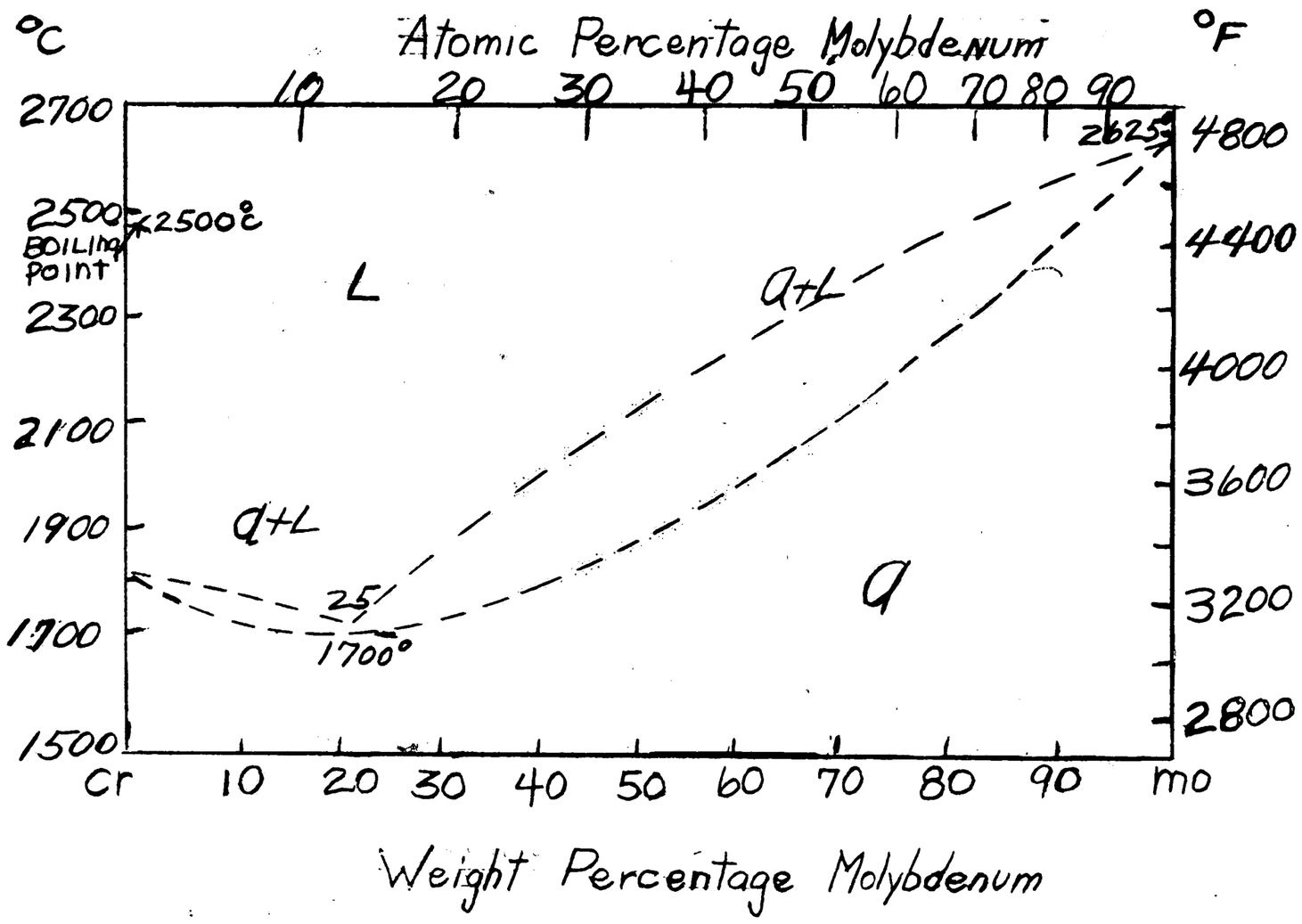

Figure 3

Chromium-Molybdenum Binary Equilibrium Diagram

(from ASM Metals Handbook 1948 Edition)

Figure 4

Chromized Molybdenum Specimen (43X)
Angle-Lapped at 1.25° Chrome Etched

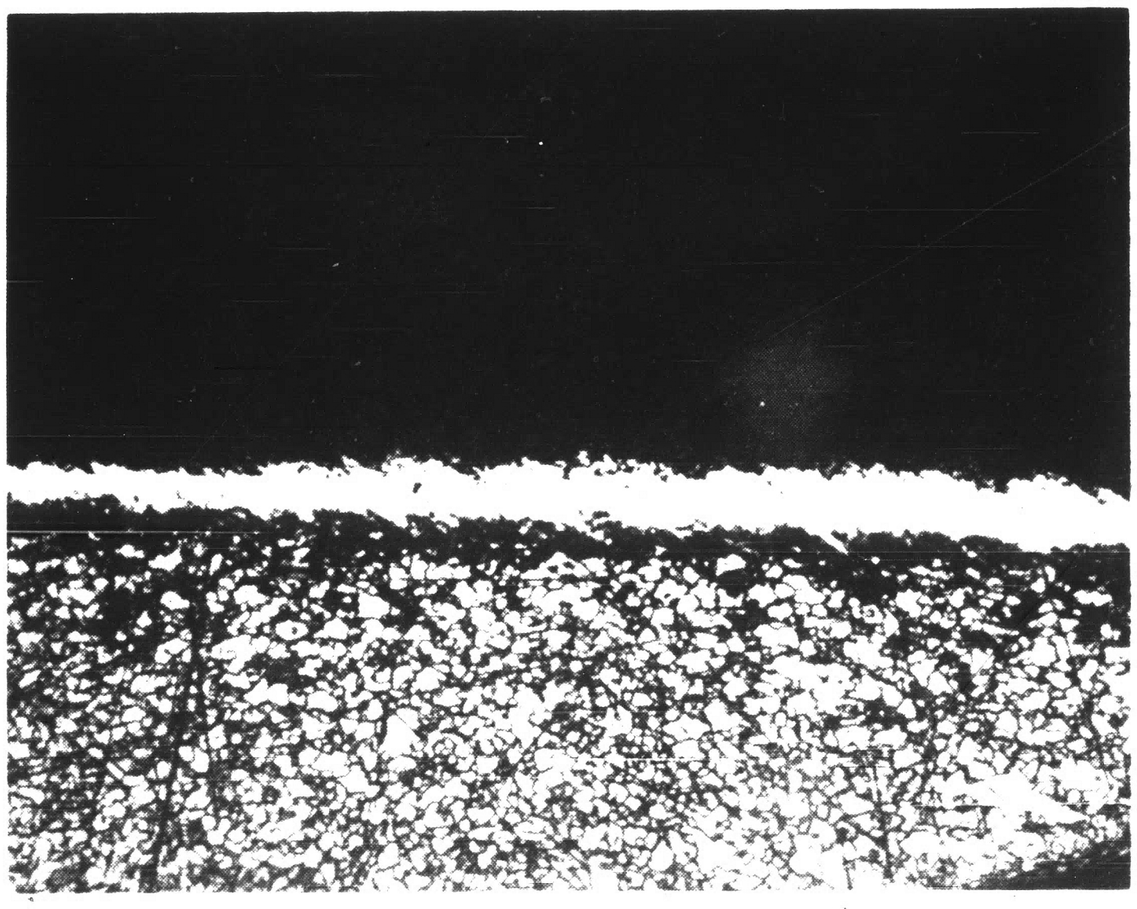

Figure 5

Chromized Molybdenum Specimen (43X) Angle-
Lapped at 1.25° Molybdenum Etched

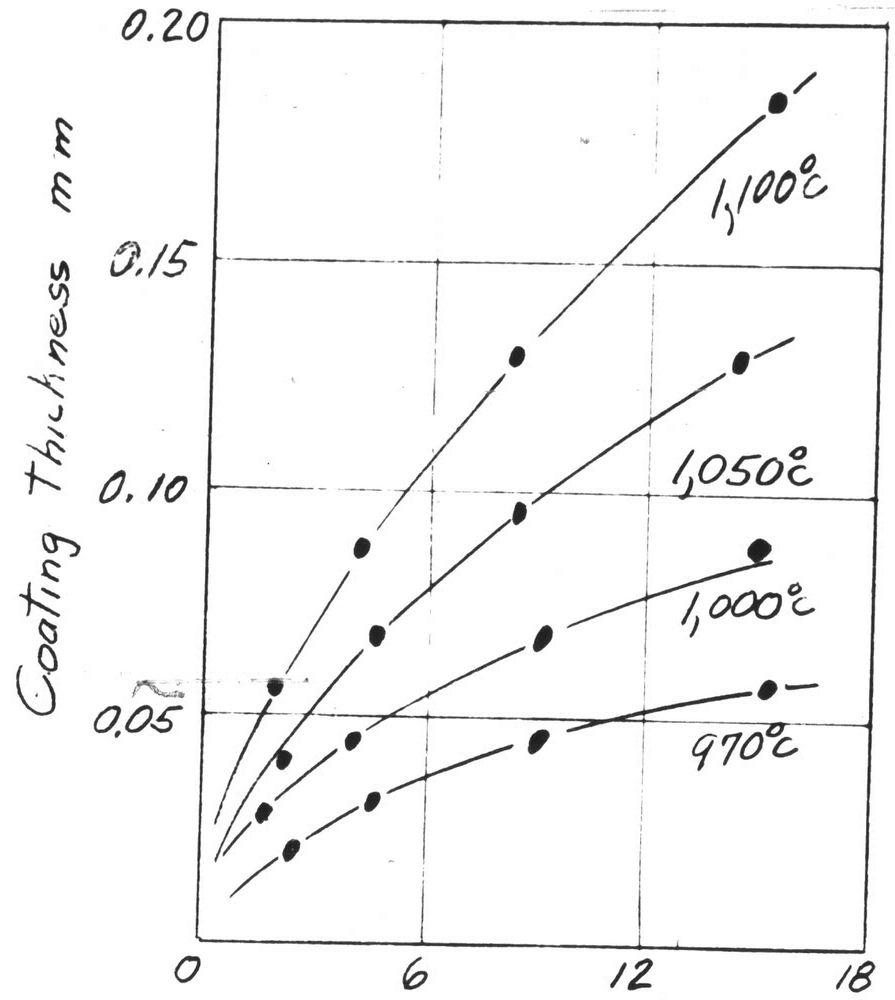

Figure 6

Variation of Case Depth with Time and Temperature
(after T. P. Hoar and E. A. G. Groom[7])

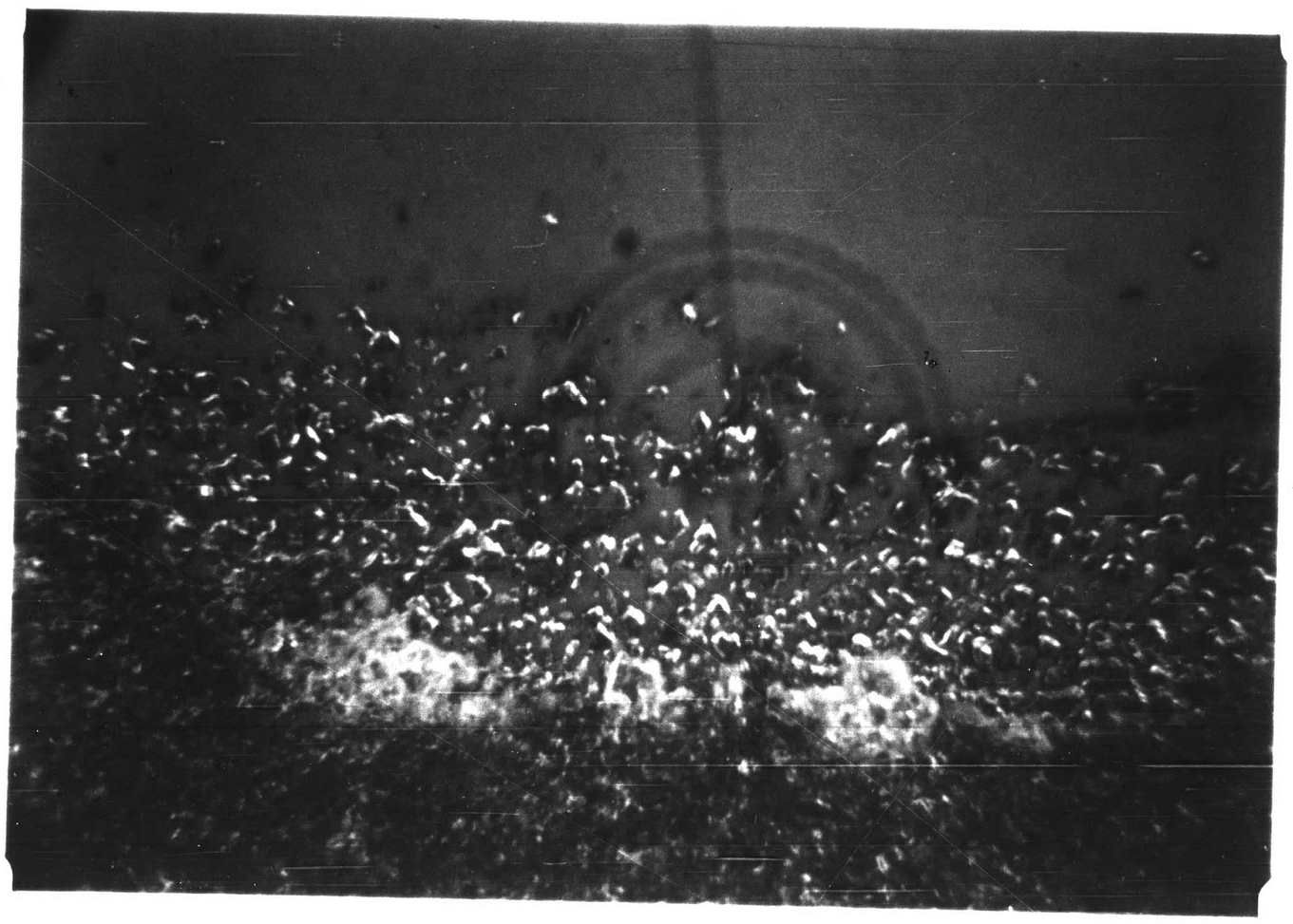

Figure 7

Polarized Light Photograph of Chromized Kovar Specimen
(500X) Angle-Lapped at 1.25°, Chrome Etched

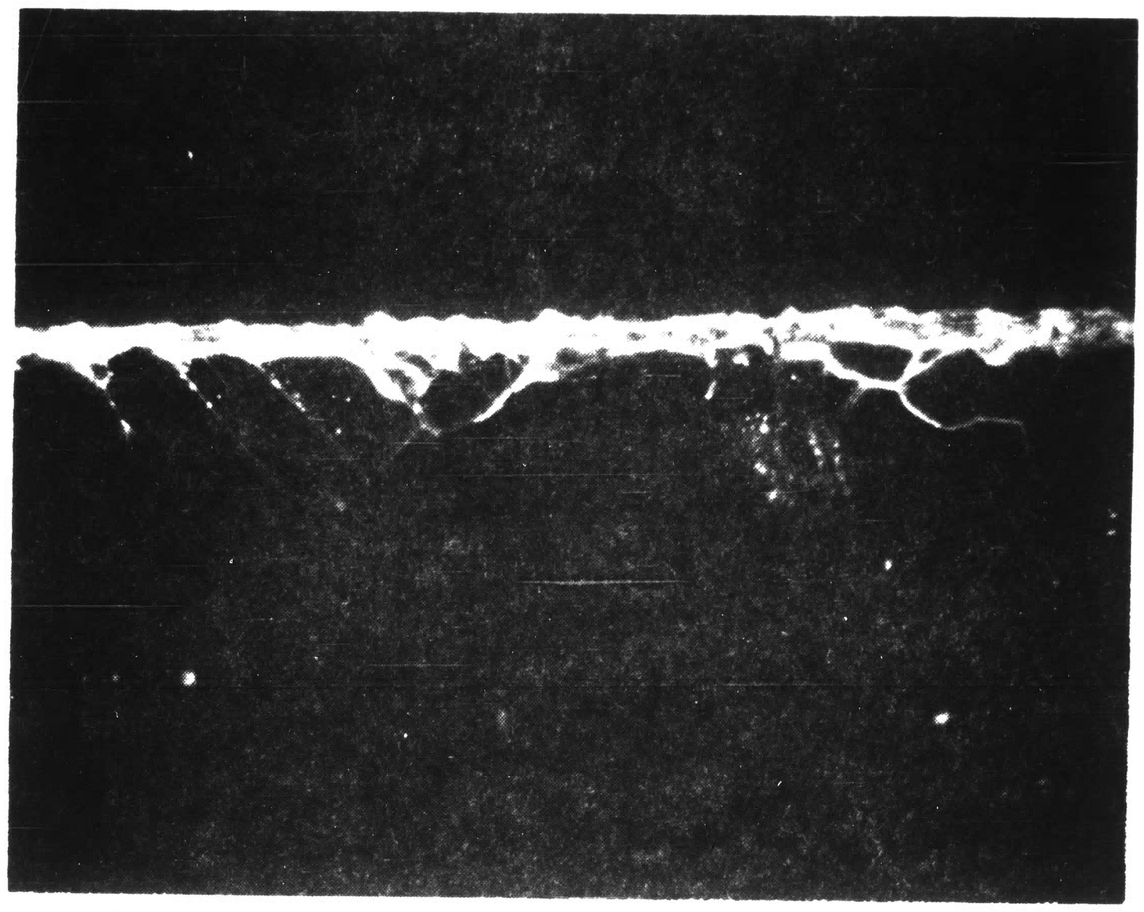

Chromi[illegible] Diffusion

Dark Fiel[illegible] Spec[illegible]
men (50[illegible] - [illegible] Stained

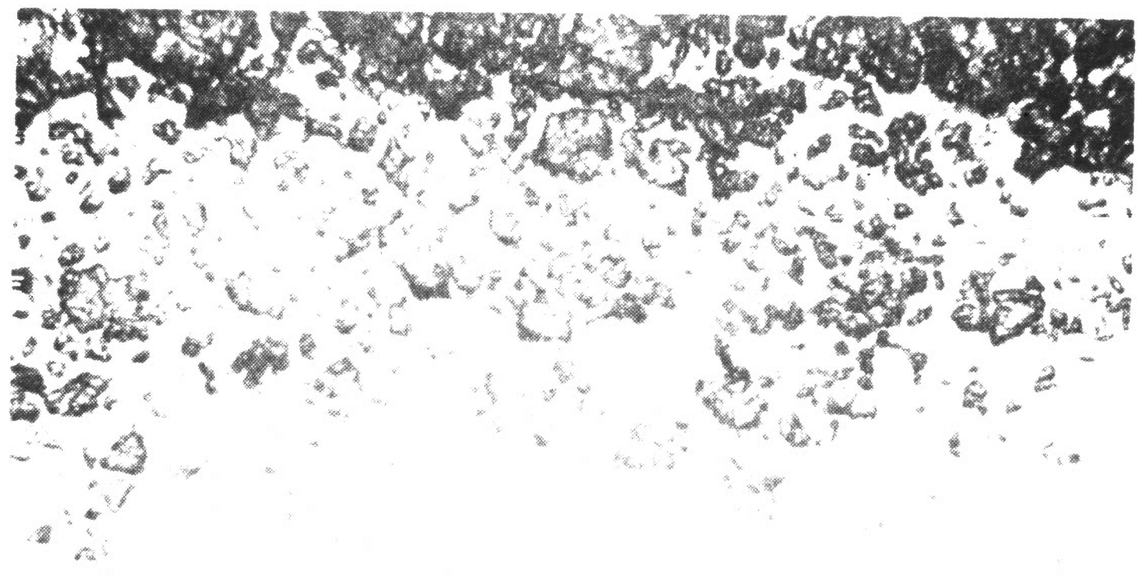

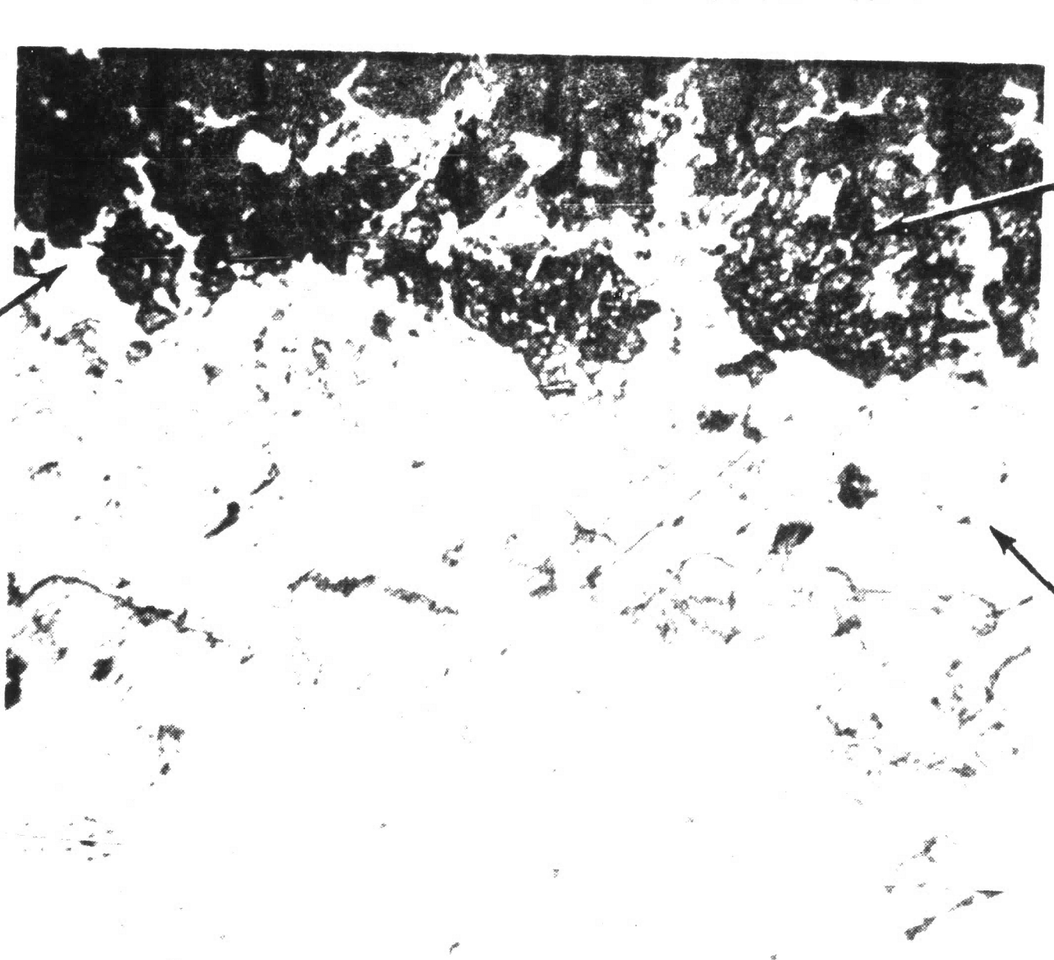

Figure
Specimen , Specimen
(, ,)

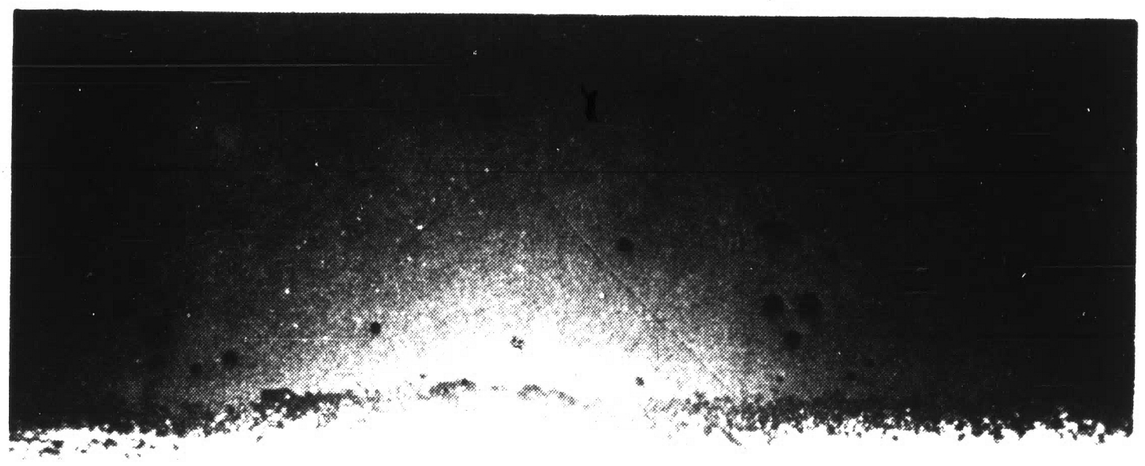

Figure 11

Preferential Chromized Kovar Specimen (25X)

Angle-Lapped at 1°, Chrome Etched

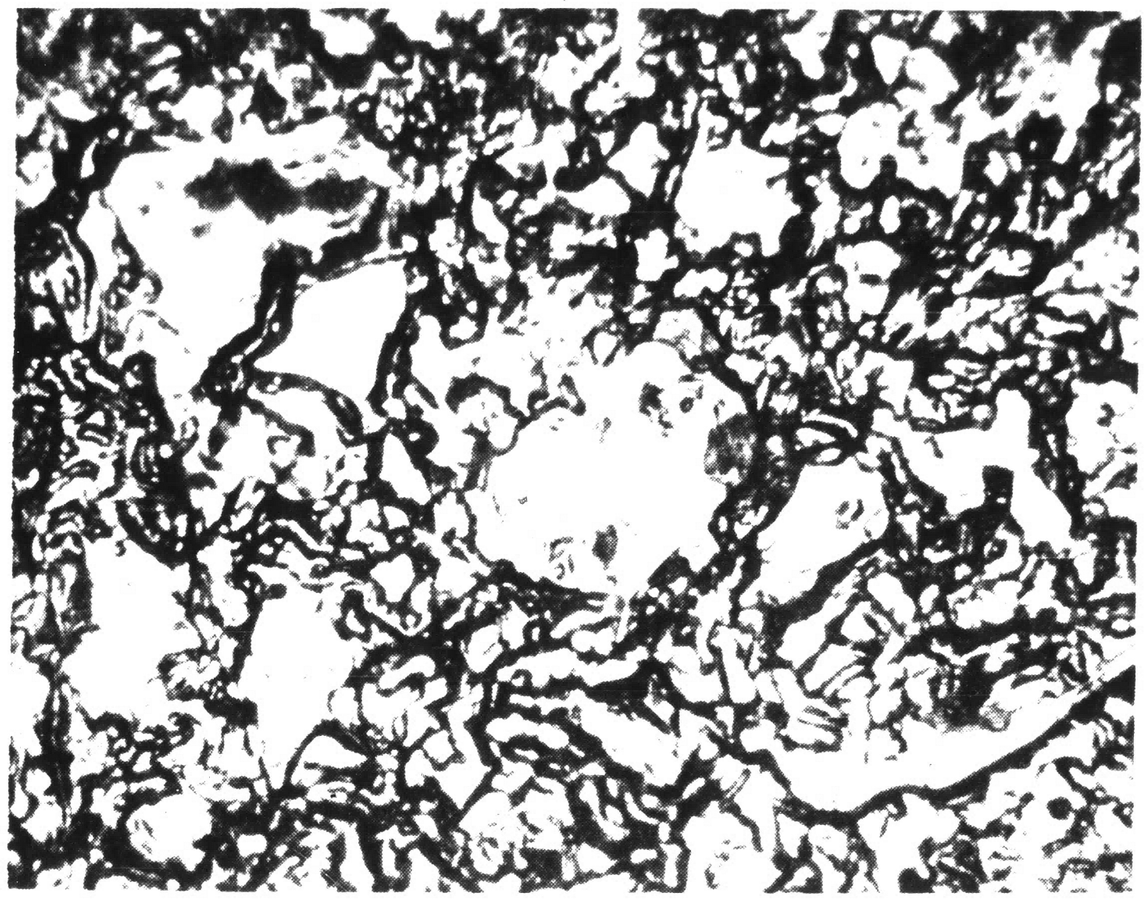

Figure 12

Surface in the Area of the Protrusion of Chromized Kovar Specimen (306X). No Etch

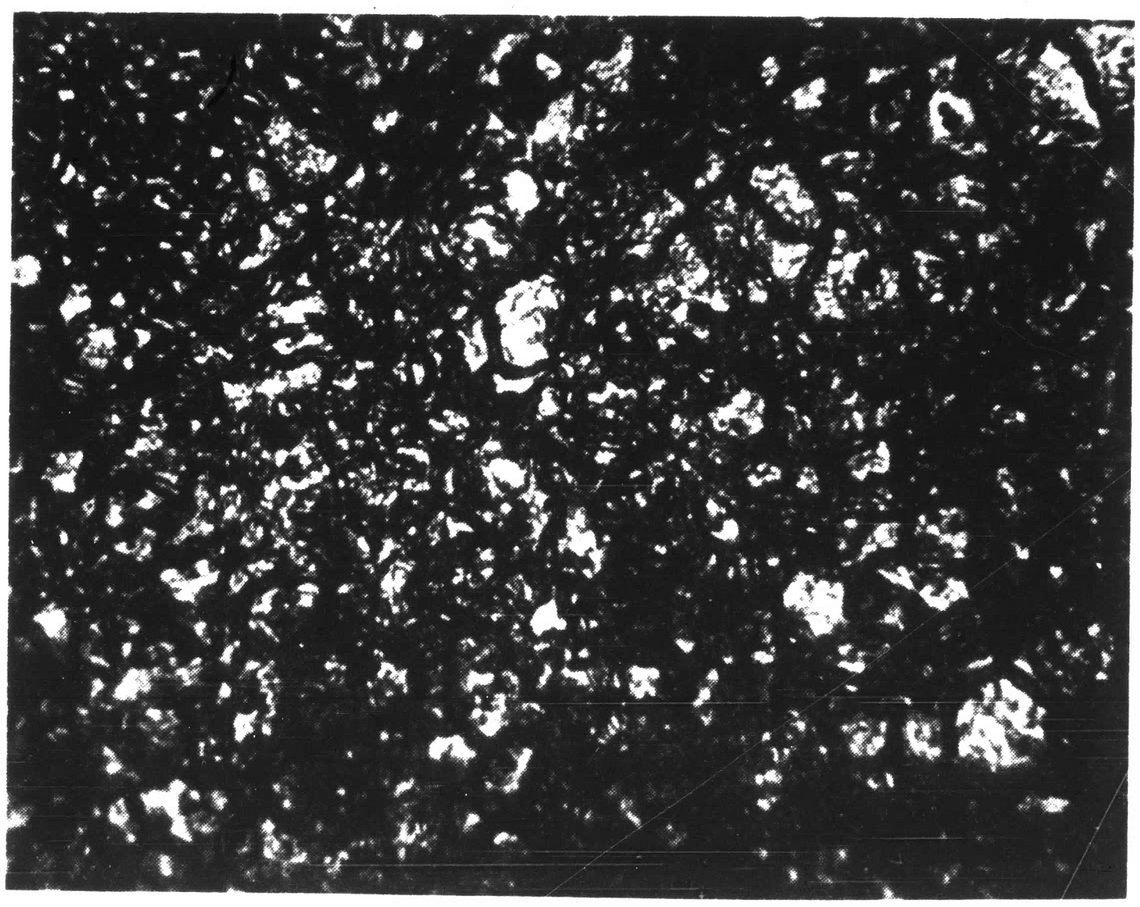

Figure 13

Surface Outside the Area of Protrusion Chromized Kovar Specimen (306X). No Etch

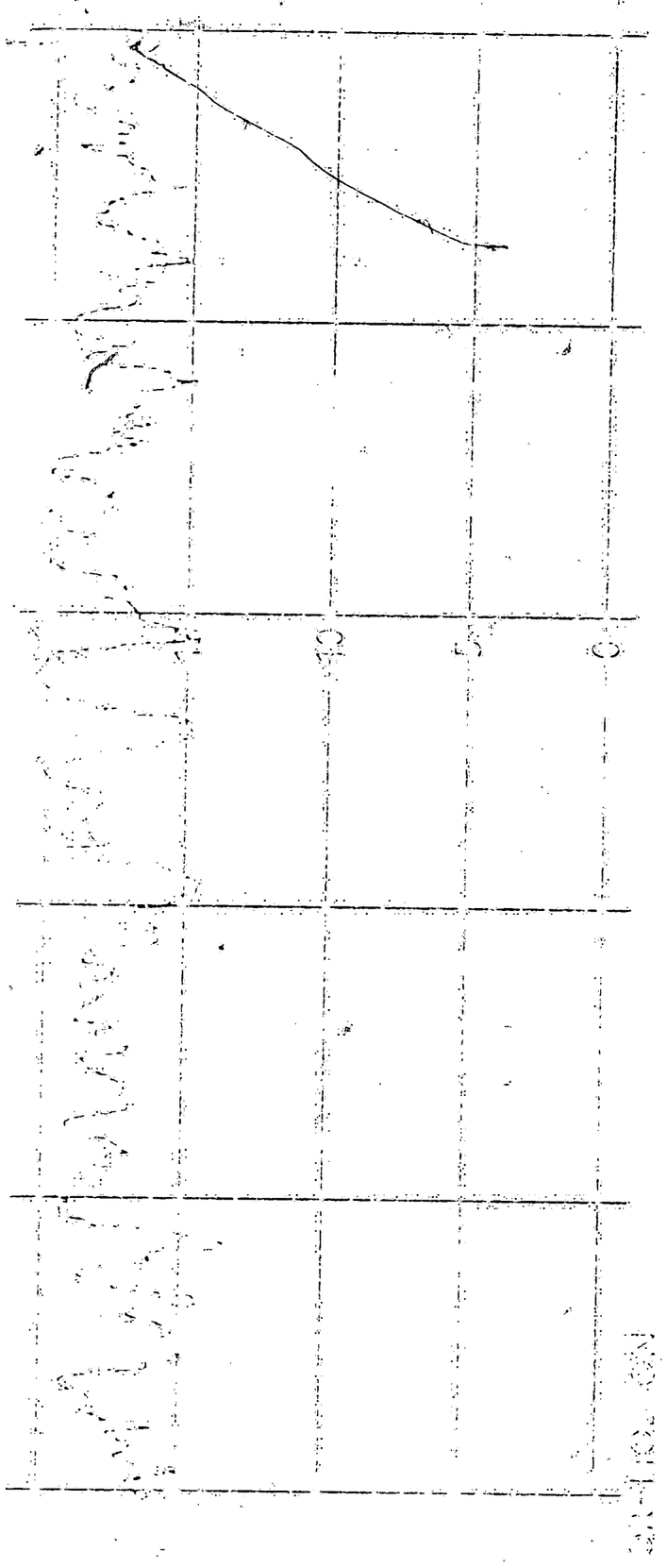

1" = 55,814 A°

Division A

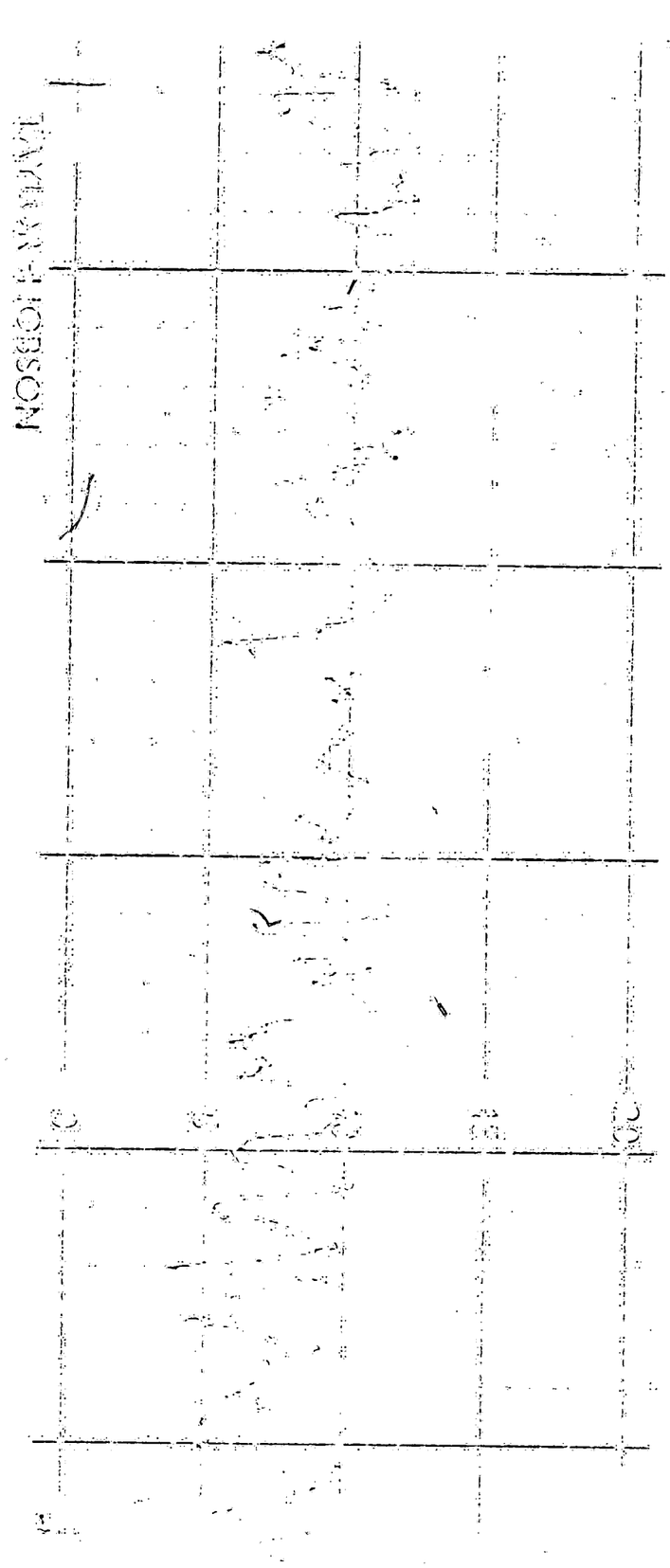

1" = 55,814 A°

Division B (⊥ A)

Figure 14
Surface Roughness Profile of
Chromized Kovar

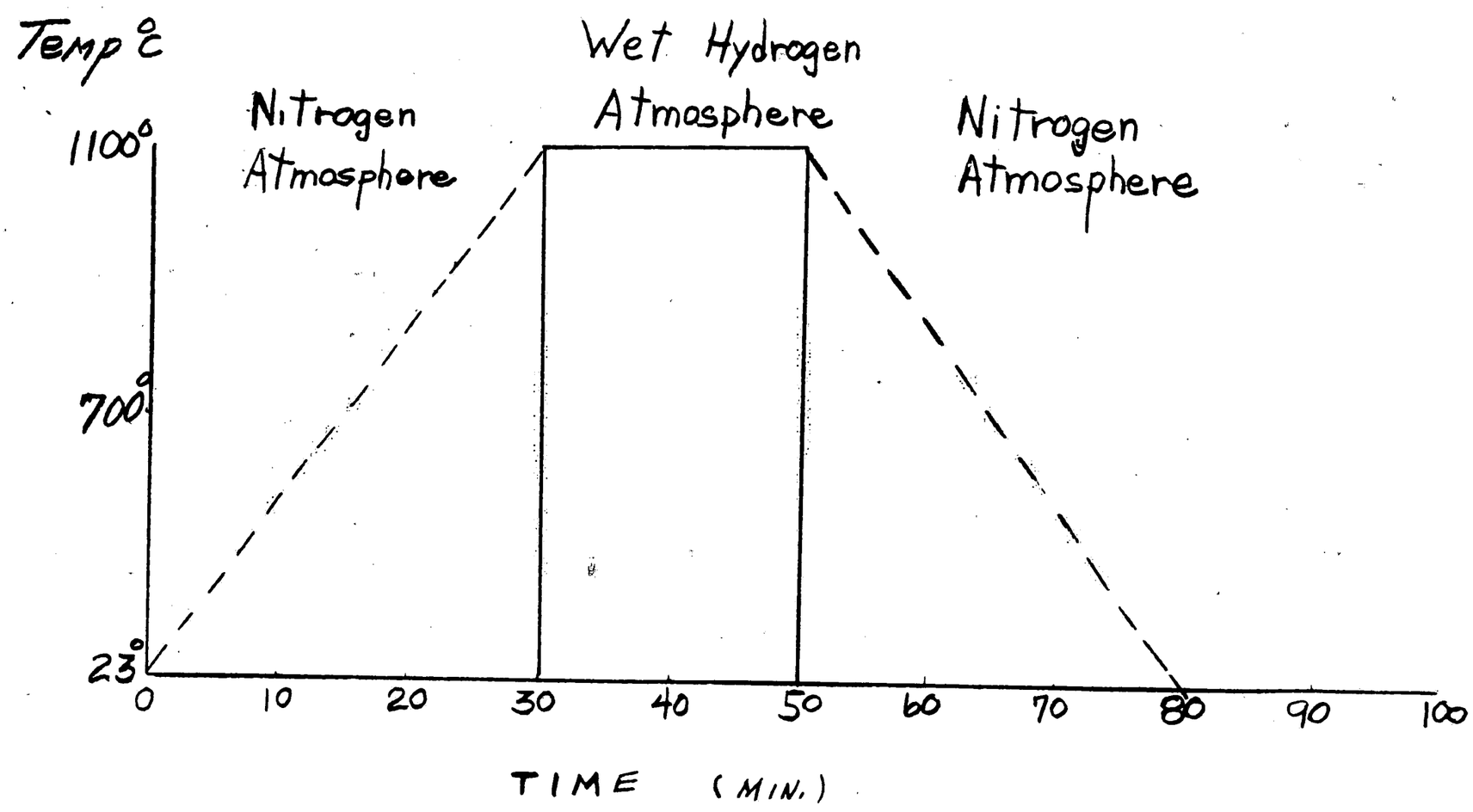

Figure 15

Typical Experimental Oxidation Run

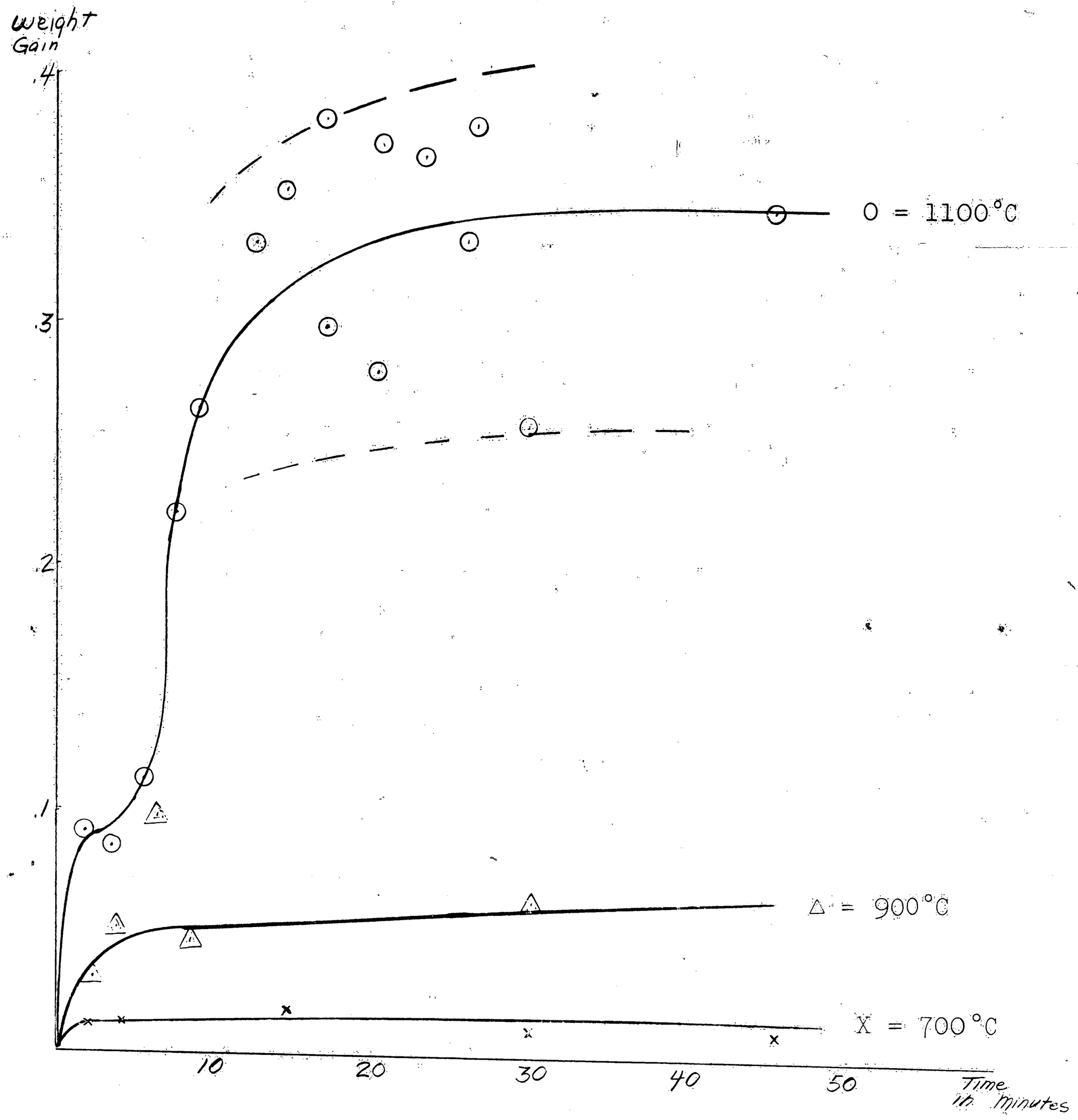

Figure 16

Oxidation Rate of Chromized Kovar in

Wet Hydrogen Atmosphere

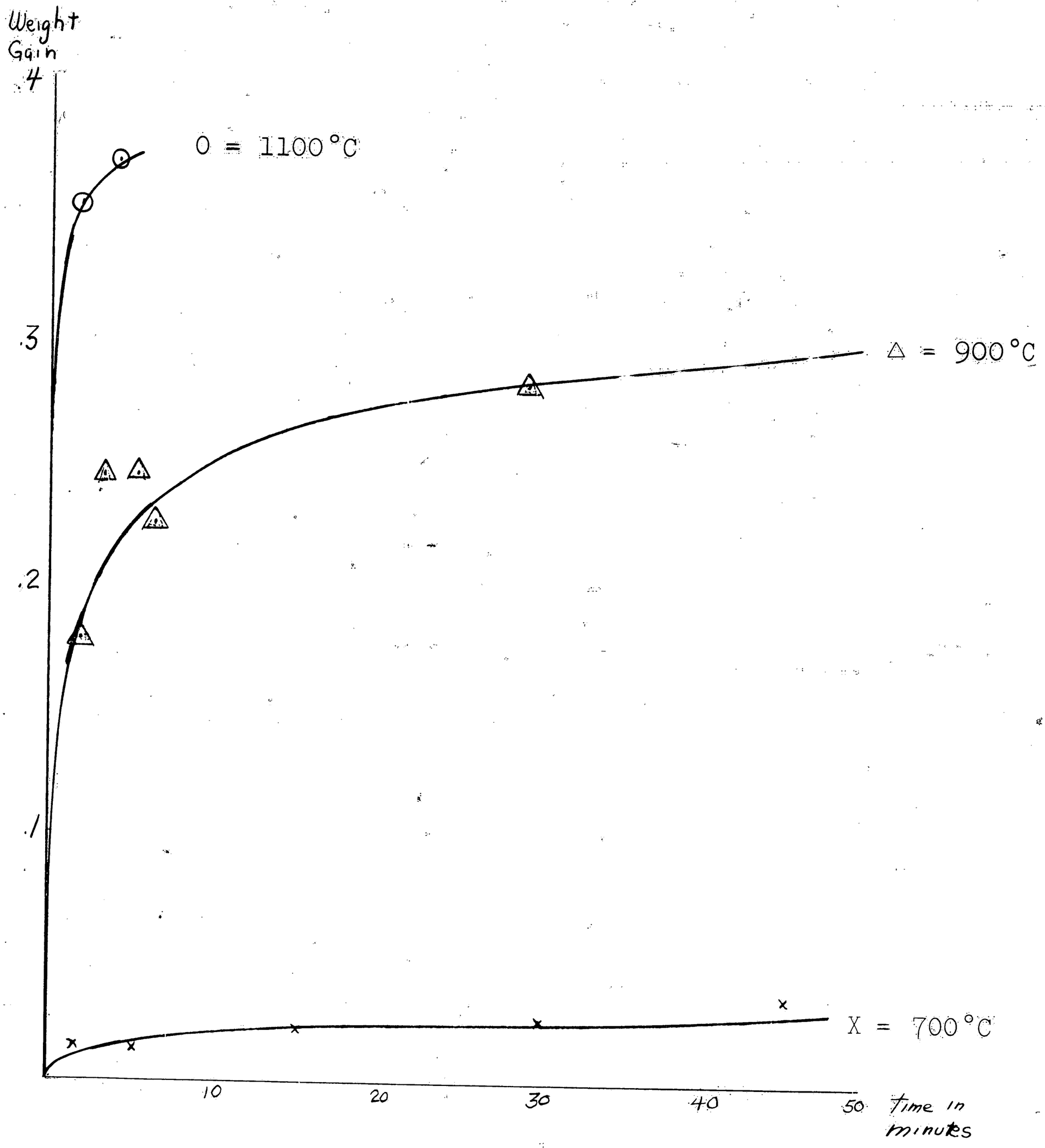

Figure 17

Oxidation Rate of Chromized Molybdenum in Wet Hydrogen Atmosphere

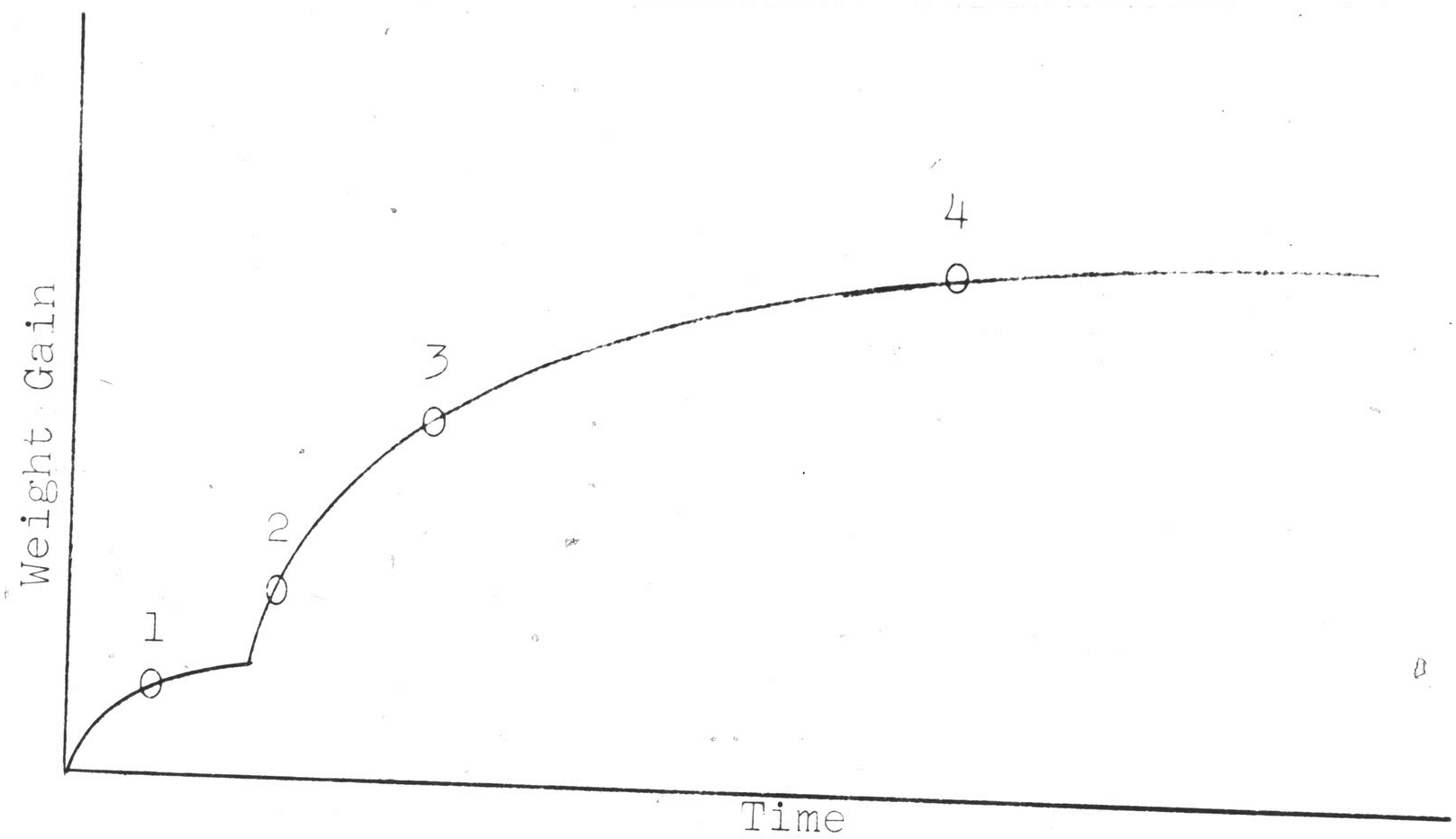

Figure 18

Idealized Curve of the Oxidation of
Chromized Kovar Showing Sample Selection

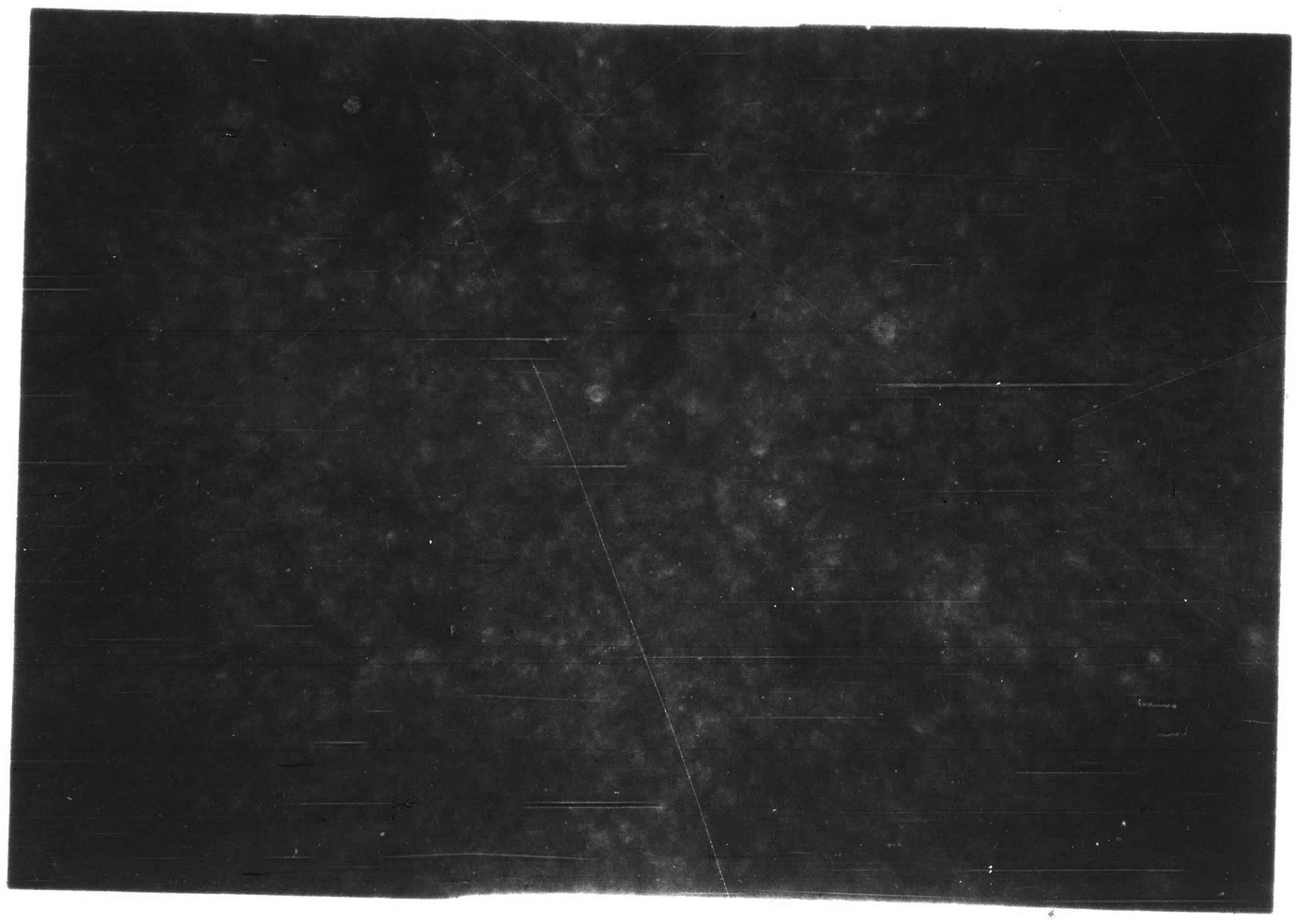

Figure 19

Polarized Light Photomicrograph (~300X) of the
Surface of the Oxide on Sample (1)

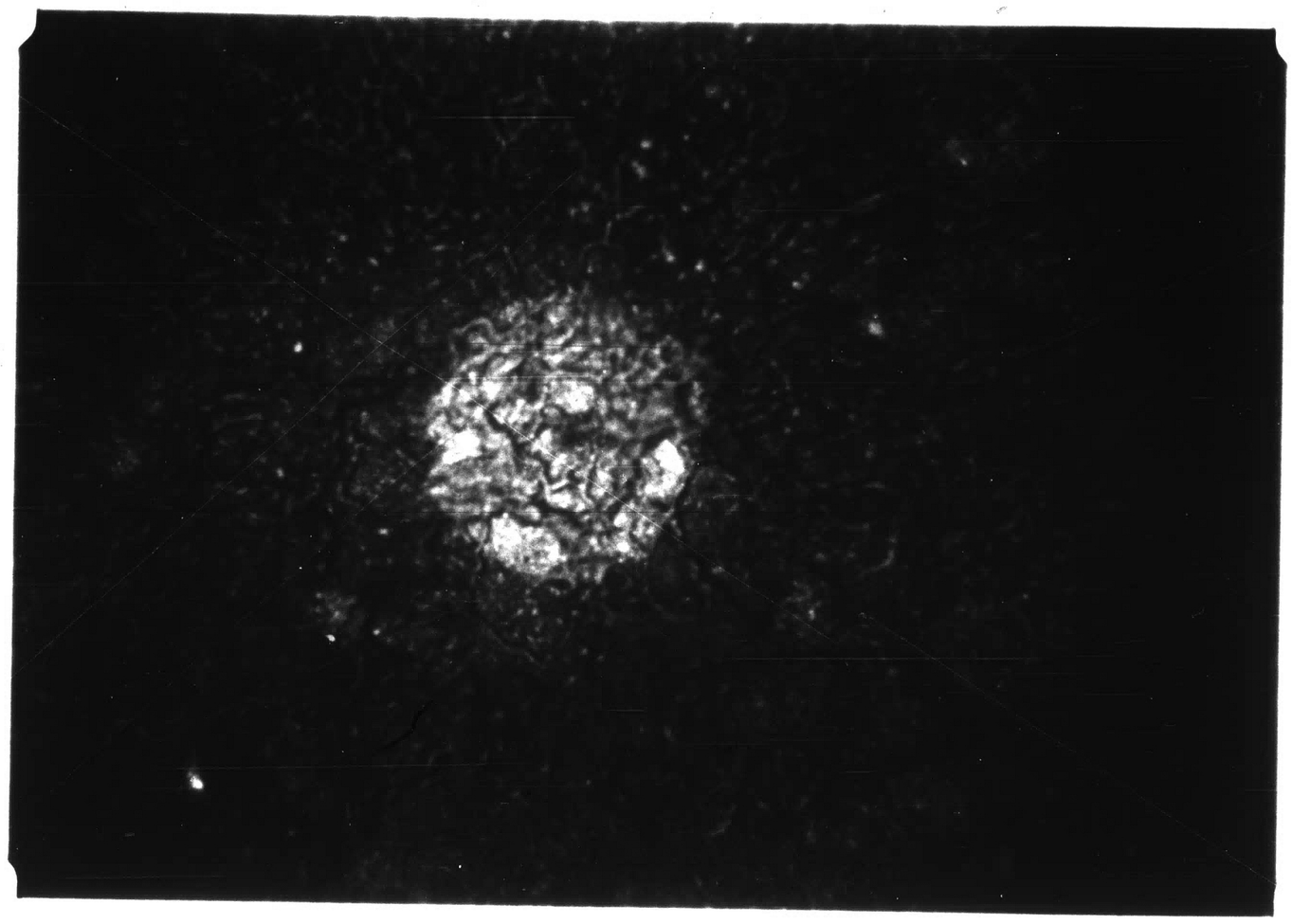

Figure 20
Polarized Light Photomicrograph (~300X) of
the Surface of the Oxide on Sample (2)

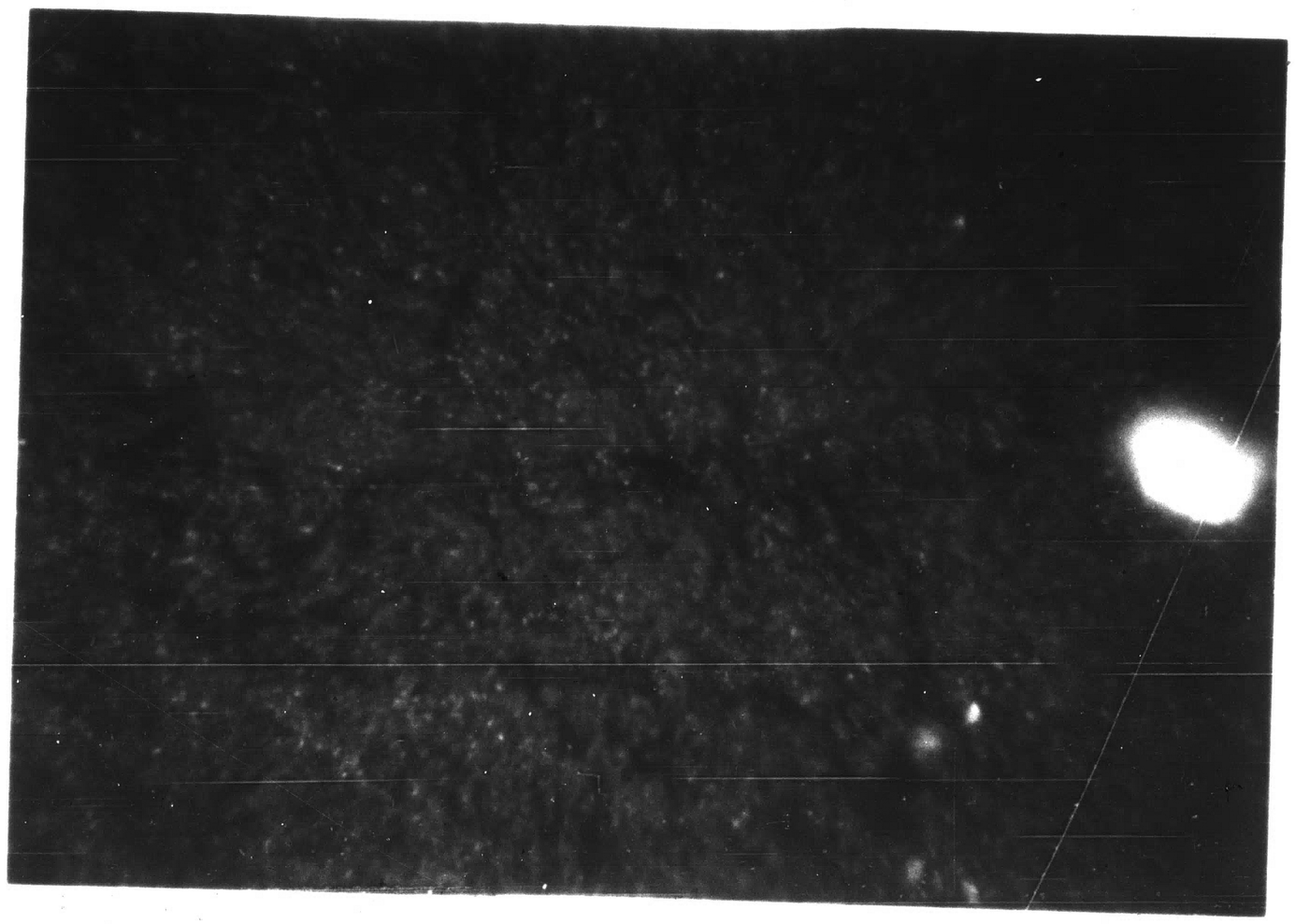

Figure 21
Polarized Light Photomicrograph (~300X) of
the Surface of the Oxide on Sample (3)

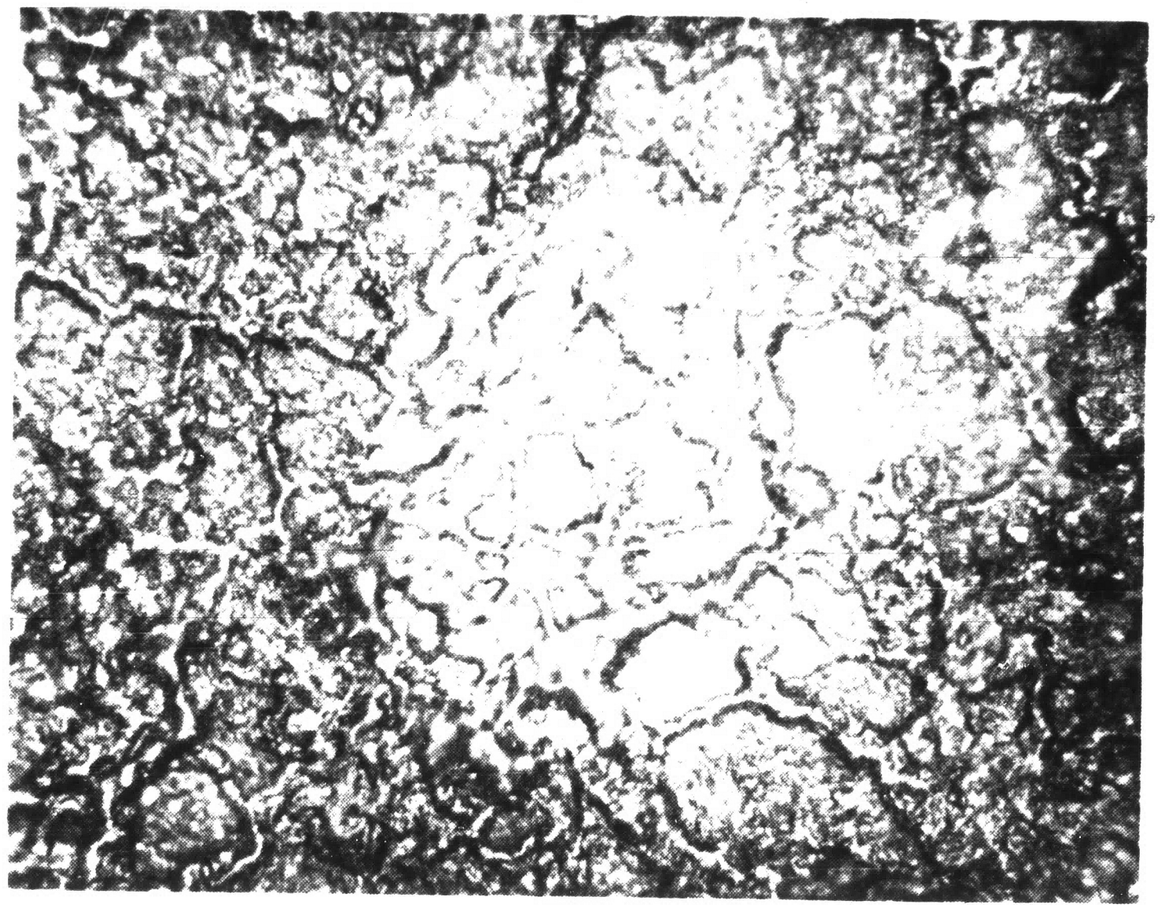

Figure 22
Photomicrograph (500X) of the Surface of the Oxide
on Sample (2) (Showing Oxide Film Cracks)

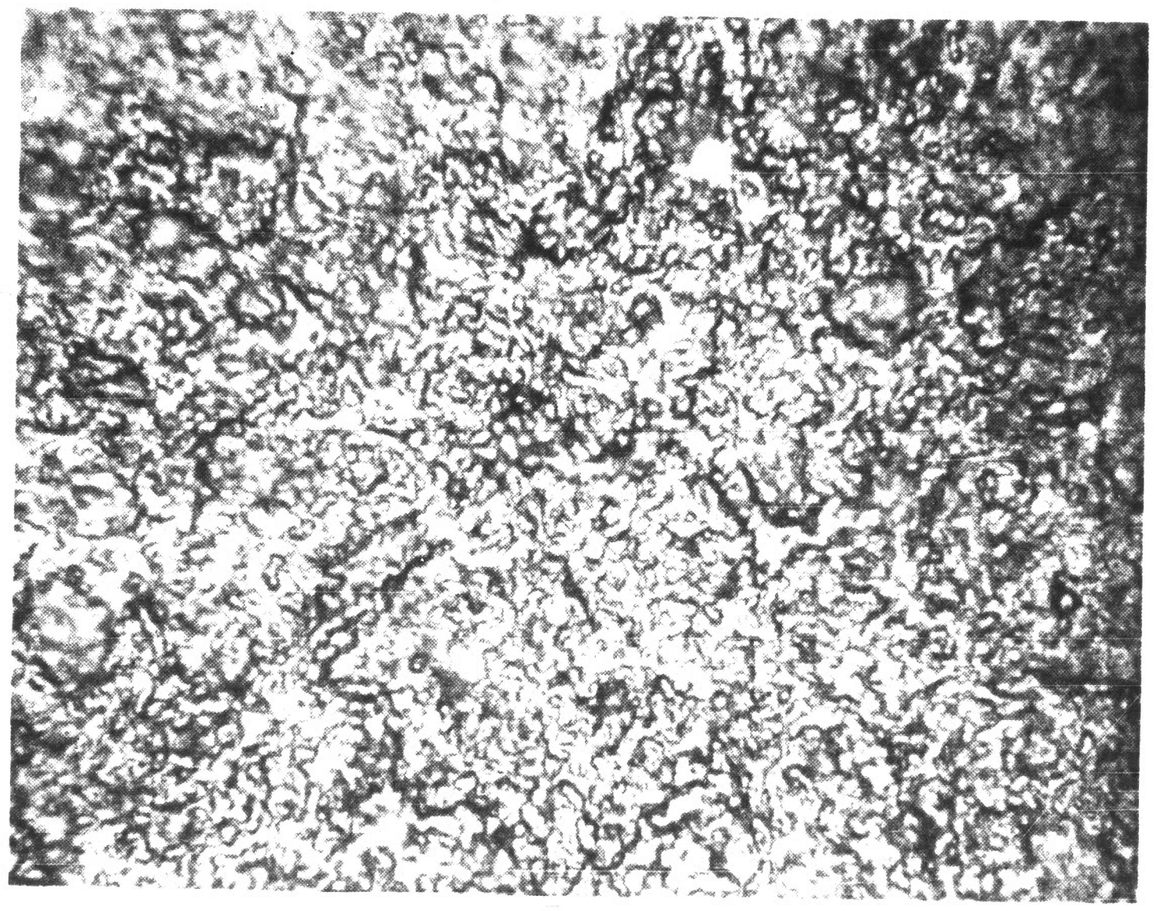

Figure 23
Photomicrograph (500X) of the Surface of the Oxide
on Sample (4) (Showing Healing of the Oxide Film)

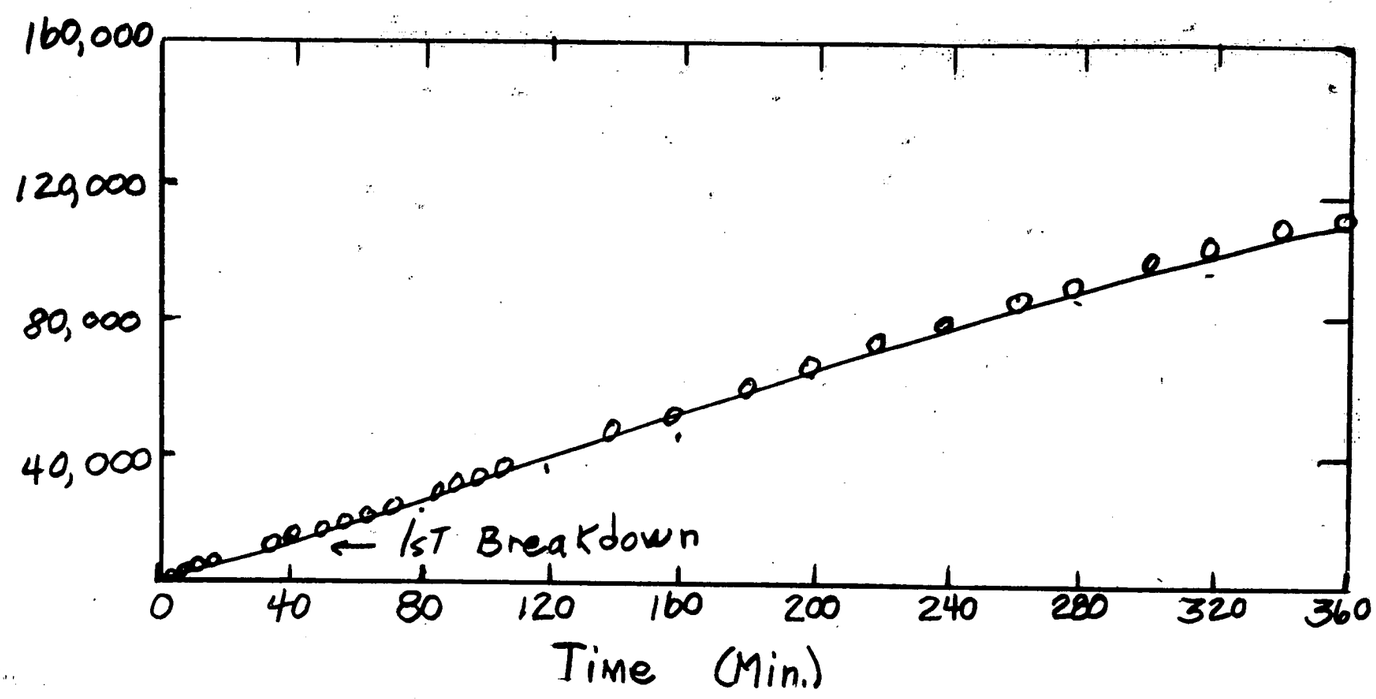

Figure 24

Oxidation Rate of Chromium
(after Gulbranson & Andrew[25])

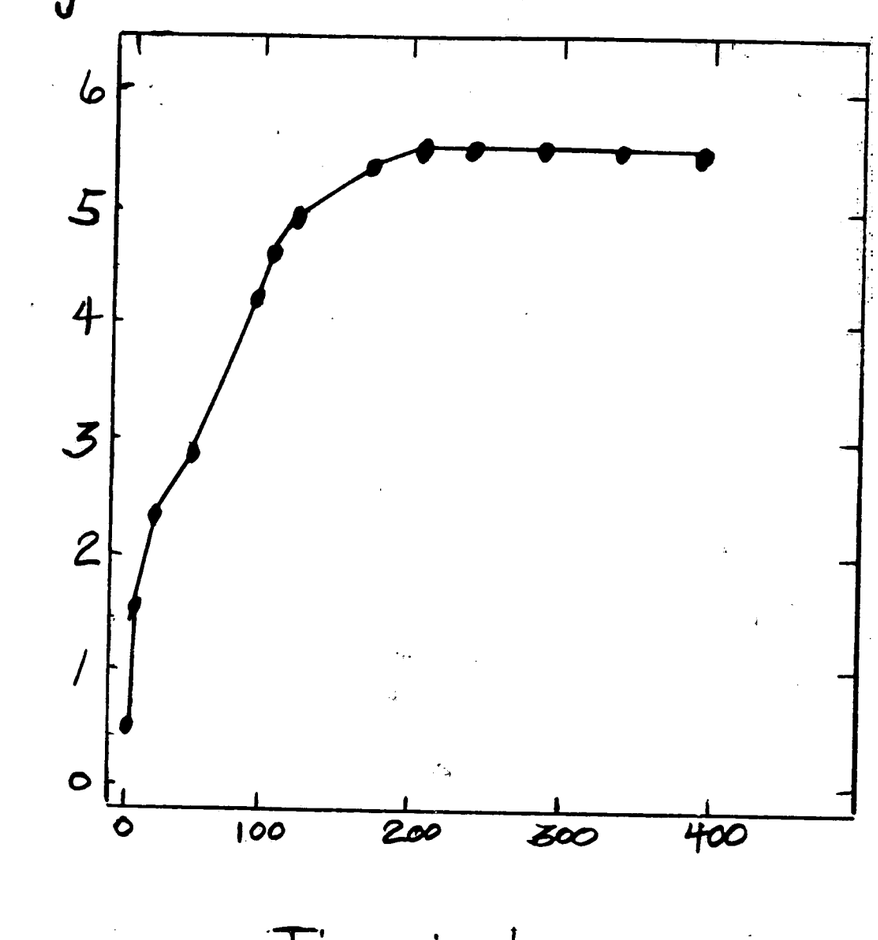

Figure 25

Oxidation Rate of Type 446 Stainless Steel
(after Caplan & Cohen[26])

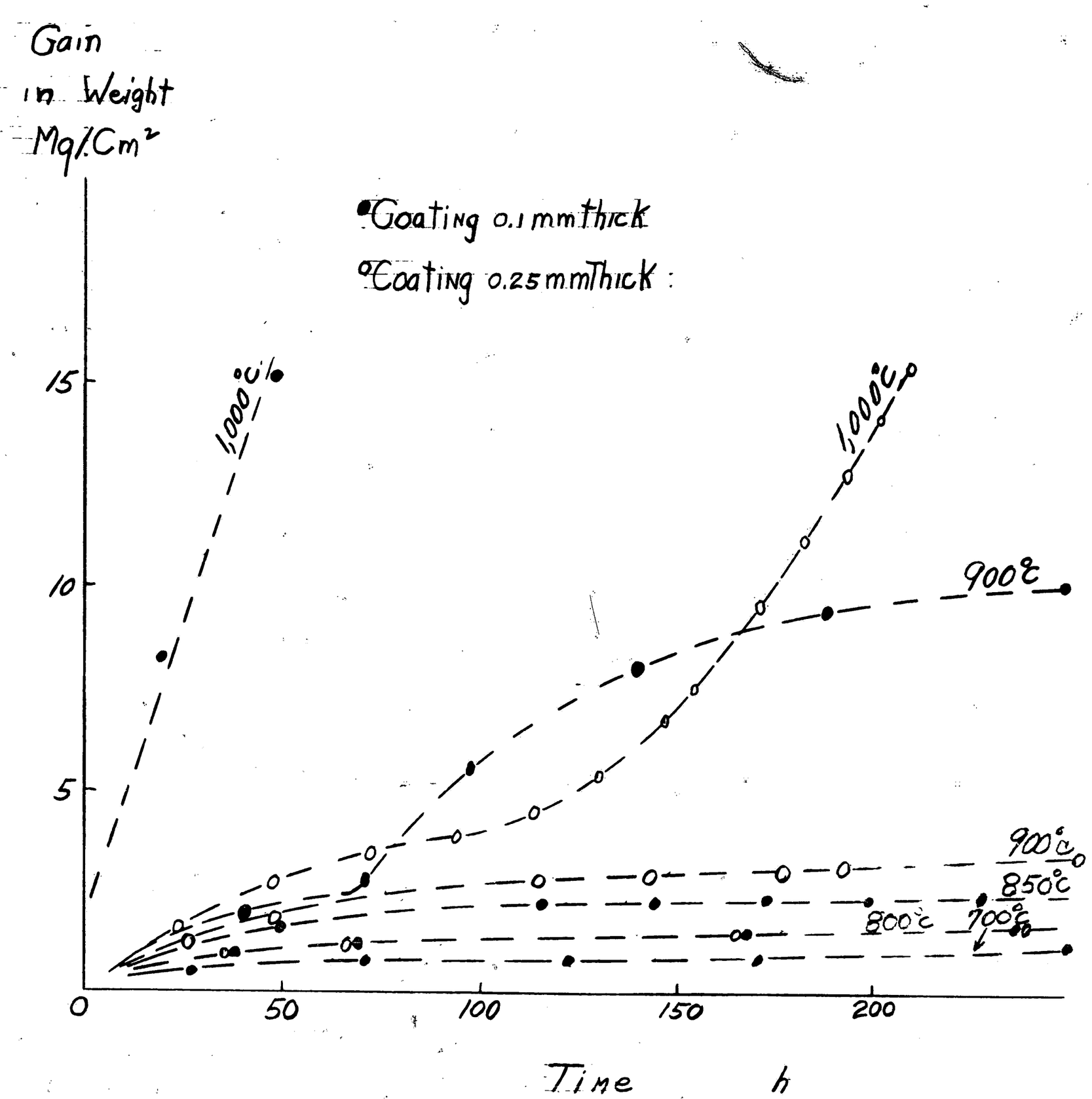

Figure 26

Oxidation Rate of Chromized Steel in Oxygen Atmosphere (after P. Galmiche[8])

Table I

Oxidation of Chromized Kovar

1100°C		900°C		700°C	
Time Min.	ΔM/A avg. mg/sq. cm.	Time Min.	ΔM/A avg. mg/sq. cm	Time Min.	ΔM/A avg. mg/sq. cm
2	.0840	2	.0305	2	.0075
4	.0775	4	.0520	5	.0085
6	.1330	6	.1020	15	.0170
8	.2250	8	.0485	30	.0050
10	.2605	30	.0662	45	.0065
12	.3310				
14	.3600				
16	.2950				
18	.3965				
20	.2700				
22	.3880				
24	.3835				
26	.3325				
28	.3950				
30	.2535				
45	.3580				

Table II

Oxidation of Chromized Molybdenum

1100°C		900°C		700°C	
Time Min.	M/A avg. mg/sq. cm	Time Min.	M/A avg. mg/sq. cm	Time Min.	M/A avg. mg/sq. cm
2	.3500	2	.1780	2	.0155
4	.3675	4	.2520	5	.0135
		6	.2500	15	.0190
		8	.2325	30	.0230
		30	.2650	45	.0460

Table III

Optical and X-ray Examination of the Oxidation of Chromium Diffusion Coatings

Sample	Optical Examination	X-ray Examination
0	Figure 10 σ phase has grown at the expense of columnar ferrite (α).	Major constituent - σ iron chromium plus σ cobalt chromium. Minor constituents - α Fe, Cr, Ni.
1	Figure 19 Relatively smooth blue-green oxide indicative of Cr_2O_3. No cracks observed.	Major constituent Cr_2O_3 or mixture of Cr_2O_3 plus α Fe_2O_3. Minor constituent CrO_2.
2	Figures 20 - 22 Cracks observed in oxide film. Possible nucleation of growth of spinel or second phase in cracks.	Major constituent Cr_2O_3 or mixture of Cr_2O_3 plus α Fe_2O_3.
3	Figure 21 Crack filling with second phase growth.	Same as above.
4	Figure 23 Complete healing of cracks retards further oxidation.	Same as above.

Biography

Thomas N. Fogarty was born on July 5, 1936, in Easton, Pennsylvania, the son of Francis J. and Catherine N. Fogarty. He attended St. Francis Parochial School and the Christian Brothers High School in St. Joseph, Missouri. He was graduated cum laude from the University of Notre Dame with a Bachelor of Science degree in Mechanical Engineering and was elected to "Who's Who Among Students in American Universities and Colleges" for 1957-1958. He received the Engineer of the Year award at Notre Dame. Since June, 1958, he has been employed by the Bell System in Allentown, Pennsylvania, and has done work in semiconductor materials, alloy transistor engineering and glass and ceramic engineering. He is an associate member of the A.S.M.E. and a member of Tau Beta Pi.